Norwegian University
of Life Sciences

Master's Thesis 2022 60 ECTS
Faculty of Biosciences

Phenotypic effects of knocking out the pigmentation related genes, *abcg2*, *bco1*, and *bco1-like* in Atlantic salmon

Brandi Nicole Kuhn
Aquaculture

Preface

This thesis is a part of the ongoing GENEinnovate project, funded by BIONÆR and the FHF-project Rød laks - genetiske effekter. This thesis aimed to investigate the relationship between genetics and filet color using CRISPR/CAS9 knockout fish lines as well as selective breeding lines.

I would like to thank my advisors, Dag Inge Våge and Jacob Seilø Torgersen. Their support and advice along the way made this thesis possible. I have learned so much and I am truly grateful for this opportunity. I would also like to thank my family, my oversea friends, and the friends I made along the way. They have shown overwhelming support and I could not have done this without them. Special thanks to Sigurd Domaas who has helped me learn RStudio and helped create beautiful and informative figures.

Norway has been welcoming and I am very honored to have been a part of the culture and traditions they experience.

Brandi Nicole Kuhn

Summary

The red muscle color is one of the main quality parameters of Atlantic salmon (*Salmo salar*). Unique to salmonids, the color comes from the accumulation of astaxanthin in the muscle, which is strictly obtained from the diet since salmon cannot synthesize it *de novo*. Despite increasingly higher dietary levels of astaxanthin, this quality trait has been slowly abating over the last decade. The diet plays a central role in the coloration together with the farming environment and genetic background which also affects muscle redness. To help understand the enigma, it is important to know how astaxanthin metabolism works in Atlantic salmon and what may affect it. Previous studies have identified that this trait to be of medium-high heritability (h^2 = 0.3-0.5), identified two QTLs (quantitative trait loci) and potential causative genes which may explain differences in astaxanthin metabolism in intestine and liver. The candidate genes included *abcg2*, *bco1*, and *bco1-like*, all of which have been knocked out in individual lines using CRISPR/CAS9. In this thesis the different phenotypes have been characterized in order to prove causality. Analysis of specimens (~200g) of each line revealed that some individuals of *abcg2*^{KO} and *bco1*^{KO} described modest increase in muscle color compared to the wild type controls, the latter line also revealed some specimens with a very pale muscle color. Knockout of *bco1-like*, however, had a large positive impact on muscle redness. These results are inline with the effect of the QTLs except for the pale *bco1*^{KO} individuals. However, it is important to keep in mind that all these are mosaic founder fish with variable degree of knockout efficacy. Hence the KO efficiency was calculated using getPCR and specimens of each line with the highest KO percentage were chosen for further analysis. Formalin fixed mid intestine and liver samples were analyzed for lipid droplet content using fluorescence microscopy. Image analysis of liver showed that there was a statistically significant increase in lipid accumulation for all the KO lines, and that lipid droplet size was also affected. For liver, only *abcg2*^{KO} fish described steatosis, with an increase in lipid load and droplet size. RNA sequencing and differential gene expression (DEG) analysis was carried out in the intestine and liver samples of the KO fish. In addition, corresponding samples from salmon genetically selected to be either red or pale was included in the analysis. The most important findings from DEG came from *abcg2*^{KO} mid intestine and *bco1*^{KO} liver. While the other KO fish showed no changes in gene expression. The *abcg2*^{KO} mid intestine had 1726 genes showing differential expression with several regulated networks involving cholesterol and steroid biosynthetic processes. In addition, four genes involved in carotenoid metabolism were found moderately upregulated (logFold2 change 1.0-1.3; 1-*apoA1, carm1, jun and*

rdh12). In the liver of the *bco1*^{KO}, there was upregulation of lipid metabolic processes and metabolism with genes involving hypoxia were regulated both ways.

In summary, phenotyping the *abcg2*, *bco1*, and *bco1-like CRISPR/CAS9* knockouts showed that *bco1-like* affects the muscle redness, with a considerable increase in color intensity. Furthermore, all investigated genes are influencing in lipid metabolism and KO of *abcg2* had the greatest effect.

Table of Contents

1 Introduction

A notable characteristic of Atlantic salmon (*Salmo salar*), from here on out referred to just as "salmon", is their red-pigmented muscle, which is caused by the deposition of the carotenoid, astaxanthin. This pigment provides health benefits such as a precursor to vitamin A (Thompson et al., 1995), increased fry survival and growth (Christiansen et al., 1995), and acts as a strong antioxidant (Bell et al., 2000; Miki, 1991; Naguib, 2000). The redder the muscle is, the more astaxanthin has been absorbed from the diet. In nature, wild salmon tend to exhibit this red hue more strongly because their diet consists of crustaceans (Jacobsen & Hansen, 2001). Pale color in salmon is becoming an increasing issue for Norwegian salmon farming (Sissener et al., 2016). The reason is unknown because even though increasing amounts of astaxanthin are getting added to the diet, the pigmentation is continuing to get paler (Aas et al., 2019).

1.1 Salmon farming in Norway

Salmon farming has been an upscale industry in Norway since the 1970s (Liu et al., 2011). Norway provides long coastlines with fjords which are ideal for seawater cages because of the low strength currents and steady water temperatures. These protected and stable waters make it so salmon can be produced year-round. Salmon is the most popular fish to farm in Norway (Norwegian Seafood Council, 2022). According to Statistics Norway (2020) in 2019, Norwegian farmed salmon contributed 1.3 million tonnes of food and brought in 68 billion NOK. The aquaculture industry (worldwide) is increasing around 2-5% per year and is expected to continue expanding (FAO, 2020). Salmon farming in Norway is important from an economic standpoint and it has room to expand. Therefore, there is a dire need to find a sustainable, yet efficient method to produce salmon.

1.2 Astaxanthin

1.2.1 Astaxanthin Introduction

Carotenoids are pigments that are commonly found in plants, animals, and algae. They are responsible for vivid colors such as red, orange, and yellow that are found in nature and are only synthesized naturally by higher plants, algae, yeast, and fungi (Goodwin, 1980). Many different carotenoids can be grouped into xanthophylls and carotenes. Xanthophylls contain oxygen in their structure whereas carotenes do not possess oxygen atoms and are composed strictly of carbons and hydrogens (hydrocarbons). The most important carotenoid found in salmon is the xanthophylls, where the most dominant xanthophylls found within the salmon muscle are canthaxanthin and astaxanthin (Storebakken & No, 1992). Astaxanthin is, however, the main cause of pigment in salmonids and will be the focus of this thesis.

The red color that is observed in the salmon comes from the accumulation of astaxanthin in the muscle (Torrissen, 1989). Other animals that have high levels of these carotenoids are shrimp, lobsters, crayfish, and salmonids. In the wild, salmon obtain the red color strictly through their diet because they cannot naturally synthesize astaxanthin (Steven, 1948). Microalgae, such as the strain *Haematococcus pluvialis* (Chlorophyceae), can synthesize the astaxanthin and can pass it down through the food chain by either zooplanktons or crustaceans (Lorenz & Cysewski, 2000; Ranga Rao et al., 2010), which are important food sources for salmonids. In nature, astaxanthin is the dominant carotenoid found in salmon, but canthaxanthin is also found. The red color that is observed in salmon is created when astaxanthin binds to the alpha-actin (Matthews et al., 2006).

The structure of astaxanthin (Figure 1) shows two rings connected by a polyene chain. The polyene chain is non-polar and the cyclic end groups are polar. This structure allows them to lie in the lipid membrane, with their end groups faced outwards towards the hydrophilic cellular membrane with their middle area in the phospholipid bilayer, this allows astaxanthin to be liposoluble and follow lipid transport (Kidd, 2011).

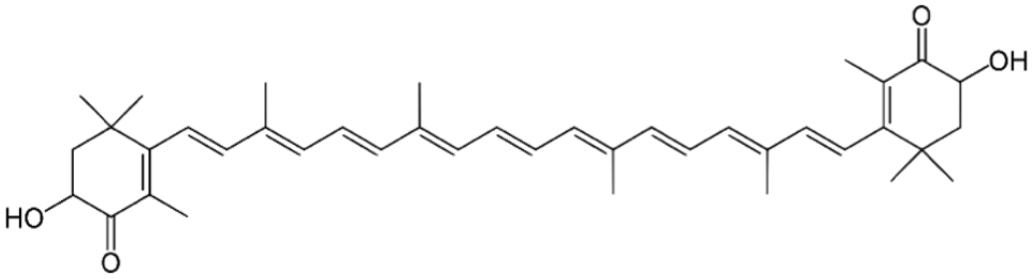

Figure 1: Structure of astaxanthin molecule. From Wikipedia page "Astaxanthin", picture by Yikrazuul, licensed under public domain.

Salmonids are known for their incredible ability to deposit astaxanthin within their flesh. White fish species such as halibut and cod do metabolize and utilize astaxanthin (Bjerkeng & Berge, 2000) but cannot deposit it in their fillets. The reasoning for this is equivocal, but it is assumed that genetics are responsible.

1.2.2 Astaxanthin Metabolism

The deposition of astaxanthin in the muscle depends on how effective the pigment is absorbed in the digestive tract. Astaxanthin gets absorbed in the mid-gut intestine (Torrissen et al., 1990; White et al., 2003) where its hydrophobicity allows it to follow lipid droplets throughout the metabolism (Clark et al., 2000; Clevidence & Bieri, 1993).

Once astaxanthin arrives in the intestine, it takes on the form of hydrophobic micelles with the help of high fatty acid levels (Borel et al., 1996). The polarity of the astaxanthin lets itself be lined against the wall of the intestine and this assimilation allows it to secrete through to the enterocyte where low-density lipoproteins, called chylomicrons, take up the astaxanthin (Zaripheh & Erdman Jr, 2002). The chylomicrons then transport the astaxanthin through the blood serum (Ando et al., 1985) where it is then deposited in the muscles (Schiedt et al., 1985). The liver is the main site of astaxanthin degradation and this degradation is why only a small percentage of astaxanthin is deposited in muscle tissue (Page & Davies, 2003).

1.3 Variations in salmon flesh coloration

1.3.1 Diet

The overall diet does have an important role in color. Historically, the composition of salmon feed was mainly composed of marine ingredients. But within the last decade, the growth in the industry and demand for a sustainability has caused a shift in the feed source. With the huge demand for fish feed this growth has led to, it has become more economically beneficial to switch to a plant-based diet because it is more abundant and cheaper to obtain (Ytrestøyl et al., 2015). One negative consequence of the inclusion of plant ingredients is a low palatability causing a reduction in the growth (Torstensen et al., 2008). With fewer marine ingredients, it became necessary to add more astaxanthin into the feed to provide red color to the flesh. However, despite the increase, the color is still decreasing (Aas et al., 2019).

1.3.2 Selective Breeding

Modern breeding tools used today include phenotypic selective breeding and genomic selection. Salmon breeders can help improve the red color found in salmon by selecting parents who have above-average muscle pigmentation.

Atlantic salmon was one of the first aquaculture species to use modern breeding schemes and it still holds strong today. This is important for aquaculture businesses and can improve the overall quality of the fish as well as welfare. It does this by selecting the best fish per generation as parents for the next generation. The goal of breeding schemes is to optimize genetic gain and lessen the negative effects of inbreeding (Gjedrem et al., 2012).

Breeding focuses on healthy fish, so every generation the fish should presumably get better. For traits like flesh color, it is nearly impossible to see if alive individuals are good candidates. Family-based selection is a method that includes phenotypic information from parents and full/half-siblings at slaughter that can help determine if a certain individual should breed. Another method that can be used in combination with family-based selection is genotype-based selection. Genotype selection uses single nucleotide polymorphisms (SNP) for identifying variants (Houston et al., 2014). Genomic selection is an alternative where tens of thousands of SNPs are genotyped and associated with defined phenotypic traits in a reference population. Based on these associations, new candidates can be selected just based on their SNP genotypes, without knowing the exact genes involved. This method is often used in combination with

phenotypic-based selection (and genotyping of certain genes with known effects like those described below).

1.4 Genes known to be involved in astaxanthin metabolism (QTL studies)

Flesh color is a heritable trait (Quinton et al., 2005) and there are many QTL studies that have identified individual genes associated with color. The genes of interest are *abcg2*, *bco1*, and *bco1-like* which are described in greater detail below.

1.4.1 ATP-binding Cassette Transporters Subfamily G (Abcg2)

Abcg2 is an ATP binding cassette (ABC) transporter that hydrolyses ATP and utilizes the energy to transport lipids across membranes (Dean & Allikmets, 1995). In humans, ATP binding proteins have a role in cancer drug resistance (Gottesman et al., 2002). Their main physiological function is to protect an organism from xenobiotics, meaning it effectively filters out the foreign substances from tissues (Sarkadi et al., 2004). *Abcg2* is tightly linked to transporting lipids, including astaxanthin, from the enterocytes back into the intestinal lumen (Zoric, 2017). This means that, in theory, it can limit the amount of astaxanthin available for muscle deposition.

1.4.2 Beta-carotene 15,15'-oxygenase (bco1/ bco1-like)

Beta-carotene 15,15'-oxygenase, also known as *bco1*, is an important enzyme that catalyzes dietary vitamin A (carotenoids) into retinal. *Bco1-like* is a paralogue of *bco1*. They are both classified as cytosolic enzymes (Raghuvanshi et al., 2015) where they function in vitamin A synthesis and are known to degrade carotenoids. Both *boc1* and *bco1-like* may be involved in astaxanthin cleavage (Zoric, 2017), which if astaxanthin is degraded and removed from the muscle, then no accumulation of red pigmentation would occur. Both genes localize to a region with the best QTL for muscle color and in close proximity to each other on chromosome 26 (ssa26) (Baranski et al., 2010; Helgeland et al., 2019; Zoric, 2017). However, which of the gene products that is causative is unknown, though *bco1* is upregulated in pale salmon (Zoric, 2017).

1.5 Genome editing

Genome editing is a method used to make changes in the DNA of an organism by creating a targeted double-stranded break within the sequence. Genome editing tools include Zinc Finger Nucleases, TALENs, and CRISPR/CAS9. For this thesis, the focus will be on the latter. The DNA repair mechanisms of the cell will try to ligate the double-stranded break. Two main paths of repair might be followed, either non-homologous end joining (NHEJ) or homology-directed repair (HDR). Clustered regulatory interspaced palindromic repeats (CRISPR) is a modern gene-editing tool. It is widely used because of its high accuracy, and it is cheaper and easier to use than the previous techniques. If the gene sequence is known, any gene can be subject to modification. The main components needed to achieve CRISPR are a CAS9 protein and guide RNA. CRISPR is done by designing a guide RNA to match a specific gene. Once the gene is found, CAS9 cleaves the DNA sequence and now the gene can be edited through either deletion, modification, or addition.

Genetic mosaicism, where more than one genotype is present (edited and wild type), is subject to occur in the CRISPR specimens. This is problematic because only some of the F0 somatic cells are edited and others are not. Consequently, the phenotype will be a mix of both edited and non-edited. The reason for carrying out studies in F0 specimens is because of the 3–4-year generation interval in salmon. Furthermore, this also emphasizes that using the most efficient guideRNA is imperative.

1.6 Aim of study

This study will address the questions on candidate gene causality underlying two QTLs for muscle color. By using gene editing in combination with phenotypic registration, image analysis of target tissues and changes in gene expression, the aim is to functionally characterize *abcg2*, *bco1*, and *bco1-like* and their importance in salmonid astaxanthin metabolism.

2 Methods and materials

2.1 Sampling the fish

The salmon have been gene-edited by using CRISPR by Aquagen. They were injected in November 2020 and sampled in September 2021. The control fish and the knockout fish came from the same line, meaning that their baseline DNA was the same. They were raised in the same tank and given the same commercial diet (Supplemental Table 10) that contained 70 ppm astaxanthin. The fish were identified via passive integrated transponders (PIT) tags and were genotyped with the getPCR method developed by Li et al. (2019).

Another selection of salmon was selected for color. One line was selected for the red fillet phenotype while the other was selected for paleness. The only analysis that was performed was RNA sequencing for differential gene expression analysis.

The fish were sampled 11 months after start feeding at approximately 200g. No starving occurred before slaughter. They were anesthetized with Tricaine Methanesulfonate (MS-222) and were killed with a sharp blow to the head. They were cut from the gills, across the lateral line, and on through to the anus. The organs were carefully taken out. The mid intestine was cut, and the contents of the intestine were carefully emptied. Around 10mm intestine and liver were sectioned and put on either 10% formalin or RNAlater (Qiagen) for histological and gene expression analysis, respectively. The salmon´s fillet color qualities were measured using a Minolta Chroma Meter colorimeter (CR-400, KONICA MINOLTA SENCING, INC. Japan) which inspected L*a*b* color space. Figure 2 shows where the three Minolta readings were recorded on the salmon. Three readings were done to get an average. While the Minolta checked all L*a*b* colors, the main reading of interest was the a*, which reflects the intensity of redness which is the important quality parameter in salmon and the main interest for this thesis. The higher the a* value, the redder the salmon fillet was.

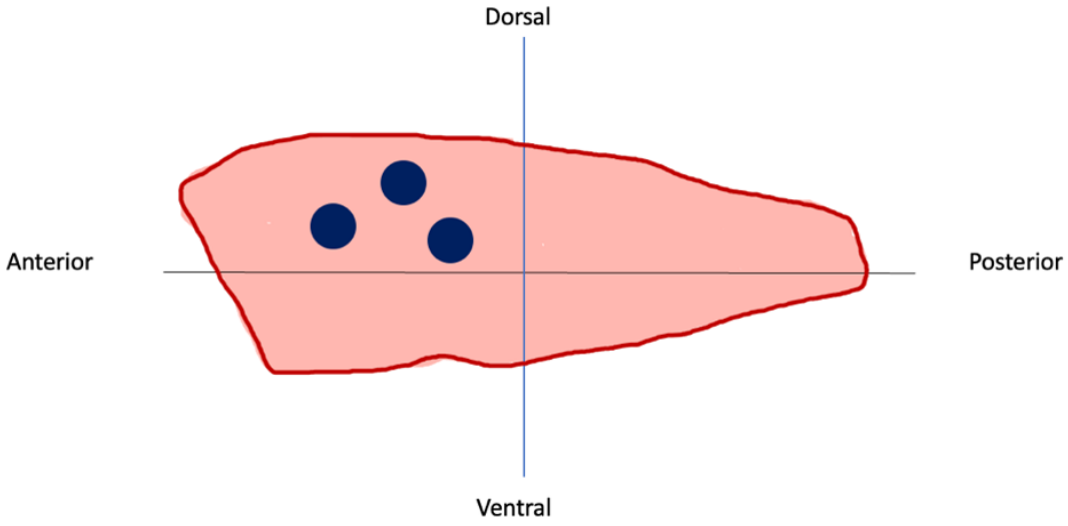

Figure 2: Sketch of salmon filet. Lines represent the orientation of the filet; dots represent the approximate location of where the readings of the Minolta were obtained. Three readings were obtained from each fish.

After recording the a* reading, it showed that the *bco1* type had readings that were lower than the lowest of the control. Those samples were then placed in a new group called "*bco1*^{KO} -low" whilst the remaining *bco1* group was called "*bco1*^{KO}-high". This separation was done to study why the *bco1*^{KO}-low was different from the *bco1*^{KO}-high. There was no need to separate the *abcg2*^{KO} group or the *bco1-like*^{KO} group.

2.2 Microscopy

Due to limited *bco1-like*^{KO} samples, they were excluded from the microscopy.

Both liver and mid-intestine tissues were used. Post formalin fixation for 24 hours, they were washed in 1 x tris-buffered saline (TBS) and stepwise dehydrated and then stored in 70% ethanol. Lipid staining was initiated by stepwise re-hydration to 1x TBS, before being rehydrated with different Ethanol concentrates (15 minutes on 50% and then 20% EtOH) and were then completed in TBS for 20 minutes. The sample was placed in a 2-3% agarose cast (agarose powder + dH_2O) and was cut in 300µm thick cross-sections using Compresstome® VF-300 and the Compresstome® VF-310 Vibrating Microtome (Precisionary Instruments Inc., Natick, USA). The best cross-sections were removed from the agarose cast and were permeabilized in a solution of TBS with 0.5% saponin (TBSS). They were then placed in a 24-

plate well and were stained overnight with the following concentrations (Table 1). Each plate was placed with one tissue sample acquainted with 100µL of the working solution.

Table 1: Staining

Product	Excitation/Emission	Staining target	Working solution
Lipid Tox Green	400/585nm	Lipids	100 x
Wheat Germ Agglutinin, Alexa Fluor™ 594 Conjugate (WGA)	600nm	Binds to glycoproteins	300 x
TBSS (0.5% saponin)	--	--	Filled to reach the desired concentration

The next day, the overnight solution in the wells was discarded and samples were briefly washed once with TBSS for < 1 minute. After the washing, they were placed in a petri dish with 1 x TBS and observed using an Axio Imager ZS microscope (Zeiss AB, Oberkochen Germany) equipped with a 40x water dipping objective. Image acquisition settings specifications are listed in Table 2. For every sample, 3 slices were obtained and stained, and inspected. There were 3 images per slice, resulting in 9 images per sample. However, due to some issues regarding quality issues, some samples could not obtain a total of 9 images.

Table 2: Target staining for fluorescence microscopy

Target stain	Laser wavelength	Laser strength	Detector gain
HCS LipidTOX™ Green Neutral Lipid Stain	488 nm	0.10 – 0.15%	700 V
Wheat Germ Agglutinin, Alexa Fluor™ 594 Conjugate	561 nm	0.10 -0.15 %	600 V

2.3 Converting microscope images

To get accurate measurements of lipid content between the different groups of fish, the fluorescence microscope images were combined with binary images of the pictures. This was done with the image processing tool, Fiji (Schindelin et al., 2012). Once a picture was inserted into Fiji, brightness was optimized based on subjective interpretation. The "subtract background" function was used (rolling ball radius 80 pixels/sliding paraboloid).

The Training Weka Segmentation (Arganda-Carreras et al., 2017) plugin in Fiji was used to train the image in separating the lipids from the background noise. A classification model was created by carefully picking between what qualified as a lipid droplet and what qualified as background. The model was tested on pictures and compared the binary image created to the original photo. Once a qualified classifier model was approved, the same model was used on all the photos. The region of interest was set to contain only the villus. It was done by creating a segmentation mask containing the region of interest. No region of interest was done on liver samples as the tissue covered the entire image field. From there the images were transformed into binary, and the images were analyzed via "analyzed particles" tool. All particles that were less than 4 pixels were excluded to reduce the background noise.

Salmon intestine and liver from the *abcg2*^{KO}, *bco1*^{KO}-high, *bco1*^{KO}-low, and control type were stained to investigate the uptake of lipid droplets. Image analyses were conducted using the 300 µm thick slices that had various target stains. The microscope, set to observe the different

wavelengths of stains, captured the lipid stain and outline of the villi (Figure 3 A+C). The binary images were created in post with Fiji and processed during Weka Training program (Figure 3 B+D), the orange outline is the region of interest where the programs counted the area coverage and number of lipid droplets. There were more droplets in the KO salmon compared to the control salmon (Figure 3).

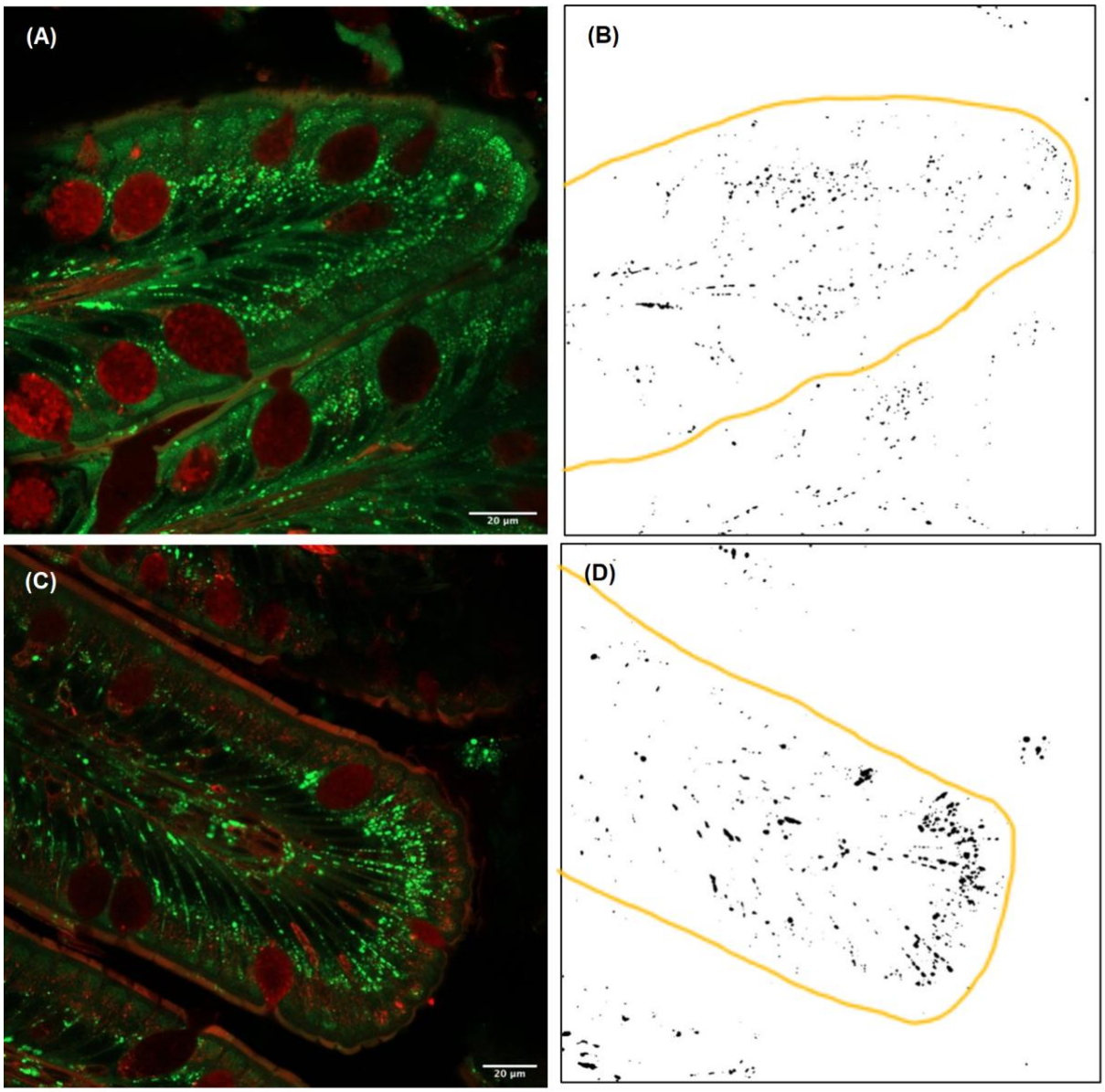

Figure 3: Images of microscope images and binary images of control (A+B) and KO (Abcg2) salmon (C+D). The orange outline in binary images represents the region of interest. More microscope and binary images of samples are available in the Appendix.

2.4 RNA extraction and sequencing

RNA extraction was done to analyze gene expression of the gene knockout groups (*abcg2*^{KO}, *bco1*^{KO}, *bco1-like*^{KO}) as well as the pale and red lines of salmon and control salmon. 10mg of the mid intestine and 10mg of the liver was extracted using MagMax mirVana Total RNA Isolation Kit (ThermoFisher Scientific, Waltham, USA) and were temporarily stored at -20C.

The RNA concentration and integrity were measured by using the 4150 TapeStation System (Agilent Technologies, Inc, Santa Clara, USA). The concentration was set to be above 25 µg/L. The RNA integrity number equivalent (RINe) was set to be above 6.0.

The samples that passed quality thresholds were sequenced by Novogene UK.

Sequence data were sent back from Novogene and subjected to a standard RNAseq pipeline to identify differentially expressed genes (DEG). The logFC value indicated how up/downregulated the genes were from which they were compared (control vs *abcg2*^{KO}, red vs pale, *bco1*^{KO}-high vs *bco1*^{KO}-low, and *bco1-like*^{KO} vs control). Only DEG that had p-values of <0.05 were included in the downstream analyses. The online tool STRING (Szklarczyk et al., 2021) was used to further identify the major gene pathways. Only >1.0 logFC and < -1.0 logFC values, along with their appropriate protein names, were used in the "Proteins with Values/Ranks" search option. Analysis of genes was created showing a network of the relationship between genes, as well as gene function. Kmeans clusters were made to separate and organize the different gene pathways. 5-6 clusters were created to investigate the most important pathways where the DE genes were involved.

3 Results

3.1 KO efficiency and a* values

Figure 4 shows the a* mean values from the control group and the KO groups. There was a total of 66 control, 108 *abcg2*^{KO}, 174 *bco1*^{KO}, and 155 *bco1-like*^{KO} samples used. Every individual had three readings of a* values and then the average was taken from those readings. All mature males were excluded from the readings since the red color is lost when fish mature because the astaxanthin is getting transferred from the flesh to the skin via a high-density lipoproteins (Bjerkeng et al., 1992).

Abcg2^{KO} had a median of 5.38, the *bco1*^{KO} and control had the lowest median averages (5.08 and 5.01 respectively), and the highest median average was *bco1-like*^{KO} at 6.36. Only *bco1*^{KO} and the control were not significant from each other (Wilcoxon pairwise test 0.96 (Supplemental Table 1)). Because some of the *bco1*^{KO} a* mean values were lower than the control, it was decided to split *bco1*^{KO} into a low and high group for further analyses.

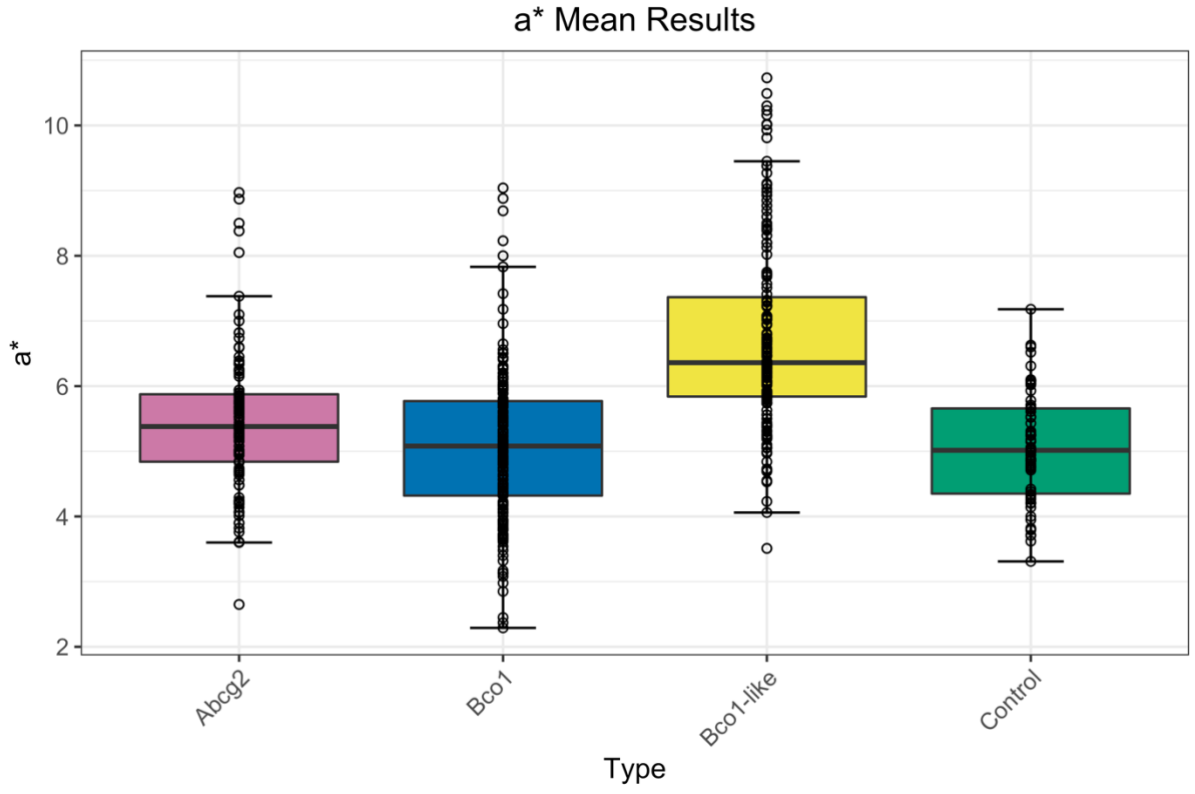

Figure 4: Boxplot of a mean values from all fish samples. It is noted that there are Bco1 values that are below the lowest control values. The bco1 was therefore split into two groups, where the low values are now being called "bco1-low "and the high values are called "bco1-high".*

Figure 5 shows the correlation between KO efficiency and a* mean values of *abcg2*^{KO}, *bco1*^{KO} low and high, and *bco1-like*^{KO}. There was a total of 16 KO efficiency numbers matched with their respected a* mean values for *bco1-like*^{KO}. When comparing the KO efficiency and the a* mean, we saw that the *bco1-like*^{KO} had most of its KO efficiency values at or close to 100%, with only a few being lower with the lowest being at 71%. At the same time, the *bco1-like*^{KO} also seems to have the highest a* mean values with the lowest being at 8.20 with no clear and non-significant correlation (p = 1.0) between the KO efficiency and a* mean (Figure 5). a* mean values from 16 sample fish from the *abcg2*^{KO} were paired with their respected KO efficiency values. When we looked at the comparison between the KO efficiency and the a* mean values for the *abcg2*^{KO}, we saw a much wider range in KO efficiency values compared to *bco1-like*^{KO} with values ranging from 39-81%. In the a* mean values we saw less of a dispersion with values ranging from 6.23 to 8.97, with a negative and non-significant correlation (p = 0.13) between the KO efficiency and the a* mean (Figure 5). Because of the differences in color tin the *bco1*^{KO} that were observed in Figure 4, it was decided to look at the "*bco1-low*" and "*bco1-high*". Starting with *bco1*^{KO}-high, there was a total of 16 readings of KO efficiency matched with their respected a* mean values. The KO efficiency ranged from 35-88%. The a* mean values were ranging from 6.14-8.88 and when paired with the KO efficiency, the correlation was weak, but not significant (p=0.82) (Figure 5). *Bco1*^{KO}-low had 12 readings of KO efficiency paired with their respected a* mean values. The KO efficiency ranged from 34–76% with a* mean values of 2.29- 3.61. There was, however, a clear negative correlation that was significant (p =0.004) (Figure 5).

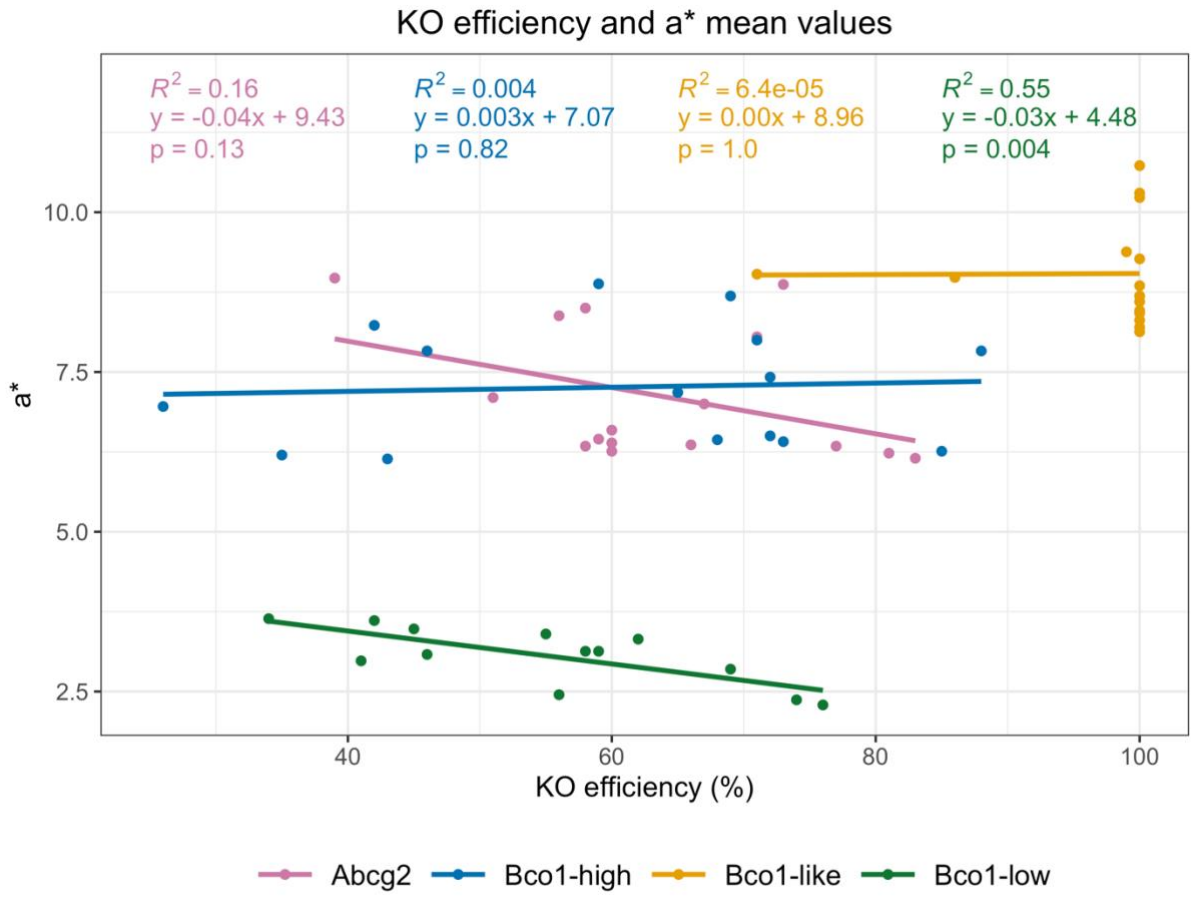

Figure 5: Correlation between KO efficiency and a mean values. a* mean indicates how red the salmon fillet was. The redder, the higher the a*. Lines represent the correlation between KO efficiency and a* mean. It is also worth mentioning the different groups observed with the Bco1 where there is clearly a population that has a low a* mean. p = probability of the slope being 0.*

3.2 Measurements of the lipid droplets in salmon

The region of the villus that was covered by lipids was compared between the control, *abcg2*^{KO}, *bco1*^{KO}-high, and *bco1*^{KO}-low for both the intestine and liver. There was a potential difference between the control and the KO groups. The KO groups showed a slightly higher median value compared to the control as well as a wider range of values (Figure 6 A). However, when looking at the liver samples, there was no clear difference in the medians, and the control group was showing a relatively high range of values compared to the KO groups (Figure 6 C). The median area coverage of the KO groups (*abcg2*^{KO}: 1.67%, *bco1*^{KO}-high: 1.01%, and *bco1*^{KO}-low: 1.27%) were not significantly different from each other (Wilcoxon pairwise test p-value > 0.08 (Supplemental Table 1)) However, they were all significantly higher than the control group median of 0.34% (Wilcoxon pairwise p-value < $1.3e^{-7}$).

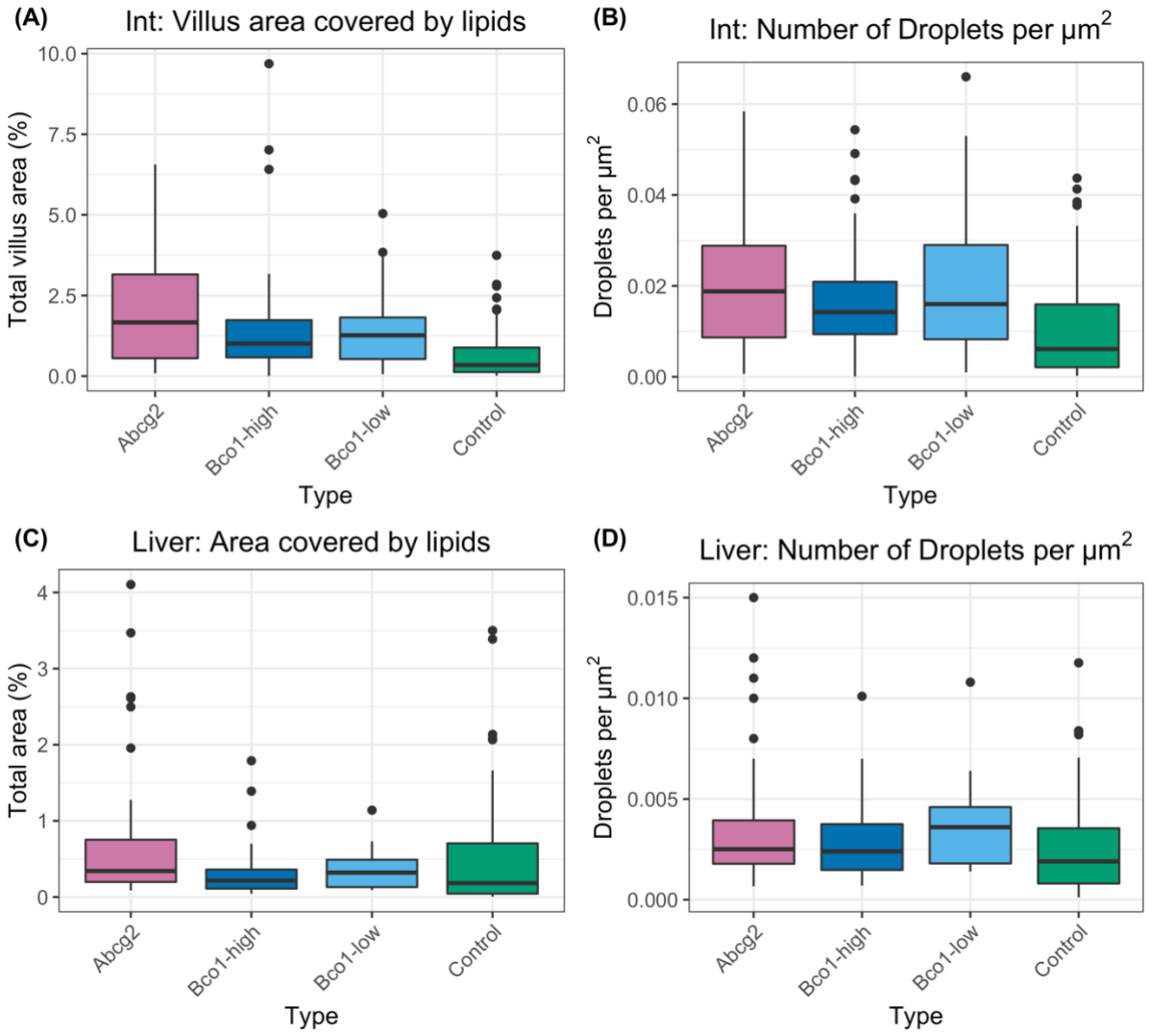

*Figure 6: Area and quantity of lipid droplets found in the KO and control type salmon. (A) and (B) represent the intestine. (C) and (D) represent the liver. Note: different scales on the Y-axis. *Int =intestine.*

The number of droplets per µm^2 was also compared between the *abcg2*^{KO}, *bco1*^{KO}-high, *bco1*^{KO}-low, and control types for both intestine and liver. As well as for the area coverage for the intestine, the median values for droplet numbers for the KO groups were higher than the control group (Figure 6 B). The droplet numbers for the liver samples showed a less clear difference between the KO groups and the control when it comes to the median droplet counts (Figure 6 D). The median number of droplets per µm^2 for the KO groups (*abcg2*^{KO}: 0.0025, *bco1*^{KO}-high: 0.0023, *bco1*^{KO}-low: 0.0036) were not significantly different from each other (Wilcoxon pairwise t-test > 0.15). In contrast to intestine samples, only *abcg2*^{KO} and *bco1*^{KO}-low were significantly different from the control median of 0.0019 (Wilcoxon pairwise t-test of respectably 0.044 and 0.032).

3.3 Intestine

For the *abcg2*^{KO}, *bco1*^{KO}-low, and control types, 85-95% of the droplets were smaller than 2µm^2. For *bco1*^{KO}-high, however, the 90% quantile was equal to 8.8µm^2, and we could see a clear bimodal distribution (Figure 7). Based on the full-size range between the control and the KO groups, the median droplet size (*abcg2*^{KO}: 0.51 µm^2, *bco1*^{KO}-high: 3.97 µm^2, *bco1*^{KO}-low: 0.63 µm^2, control: 0.34 µm^2) were all significantly different from each other (Wilcoxon pairwise test p-value < 2e^{-16}).

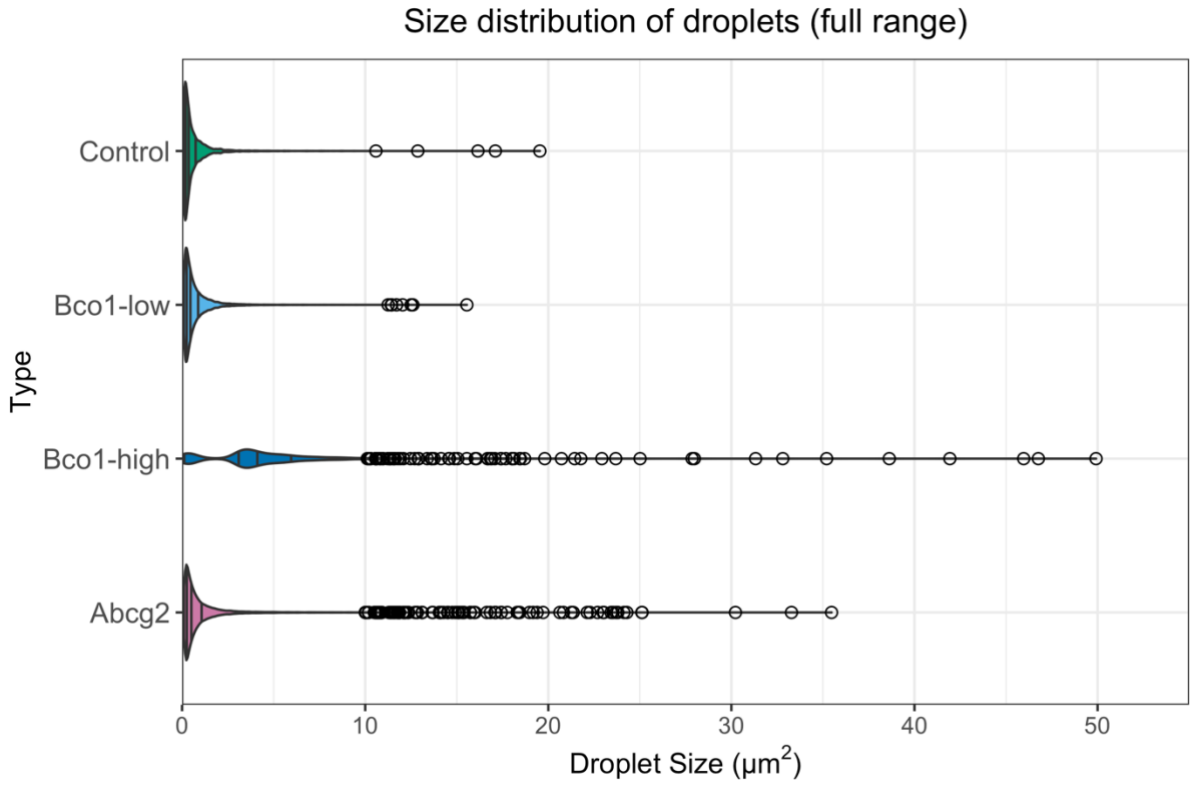

Figure 7: Full range droplet size distribution of intestine samples. Circles represent droplets over 10µm^2. A bimodal curve is observed for bco1^{KO}-high.

When looking at the full range, it was difficult to see the distribution curves between the groups. The distribution becomes clearer when the cutoff is below 11 µm^2 (Figure 8). The median droplet sizes remained ultimately unchanged (e.g., *bco1*^{KO}-high from 3.97 to 3.82), but all were significantly different from the control (Wilcoxon pairwise t-test < 2e^{-16} (Supplemental Table 6)).

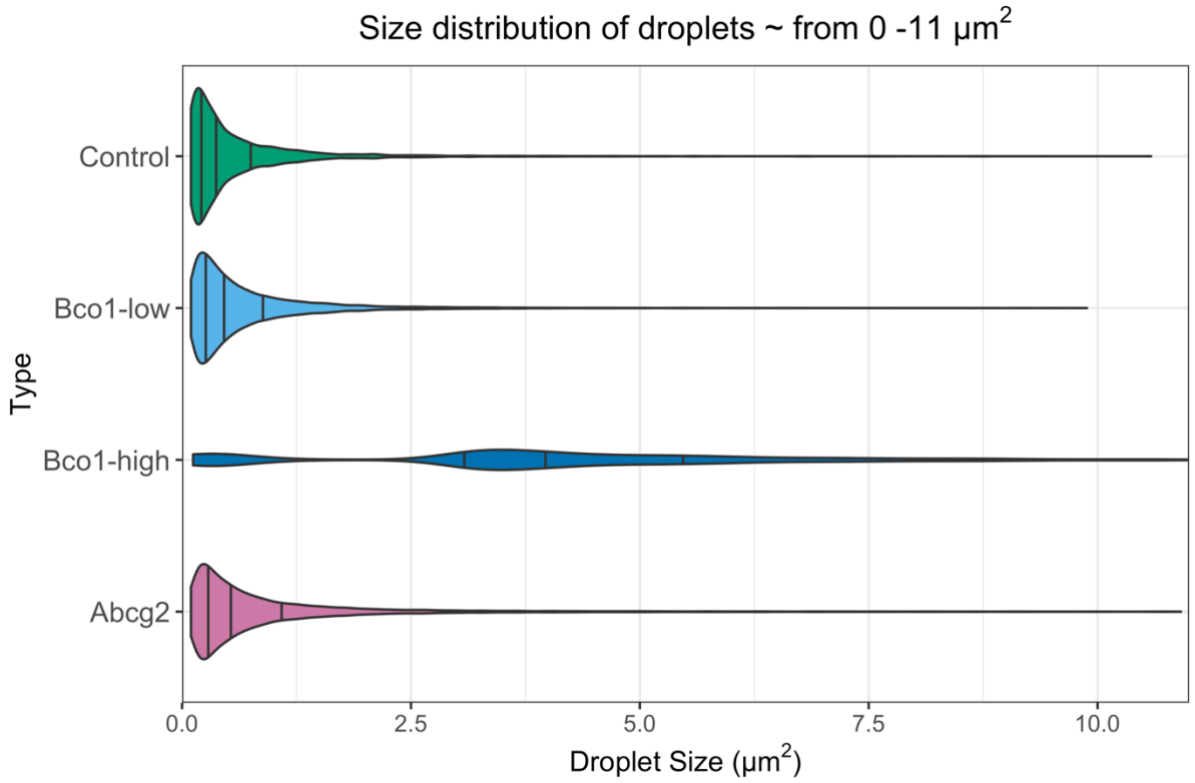

Figure 8: Droplet size (μm^2) distribution for droplets between 0-11 μm^2 for the intestine samples.

3.4 Liver

For the *bco1*^{KO}-high, *bco1*^{KO}-low, and control types, 80-85% of the droplets were smaller than 2µm^2. For the *abcg2*^{KO} type, however, the 80% quantile was equal to 7.0µm^2, and we could see a bimodal distribution (Figure 9). As seen in the intestine, a bimodal curve is also present, but this time on the *abcg2*^{KO} type. On the full range between the control and the KO groups, the median droplet size (*abcg2*^{KO}: 3.46 µm^2, *bco1*^{KO}-high: 0.46 µm^2, *bco1*^{KO}-low: 0.44 µm^2, control: 0.63 µm^2) were all significantly different from each other, except *bco1*^{KO}-high and *bco1*^{KO}-low (Wilcoxon pairwise t-test of respectively < $2e^{-16}$ and 0.16 (Supplemental Table 7)).

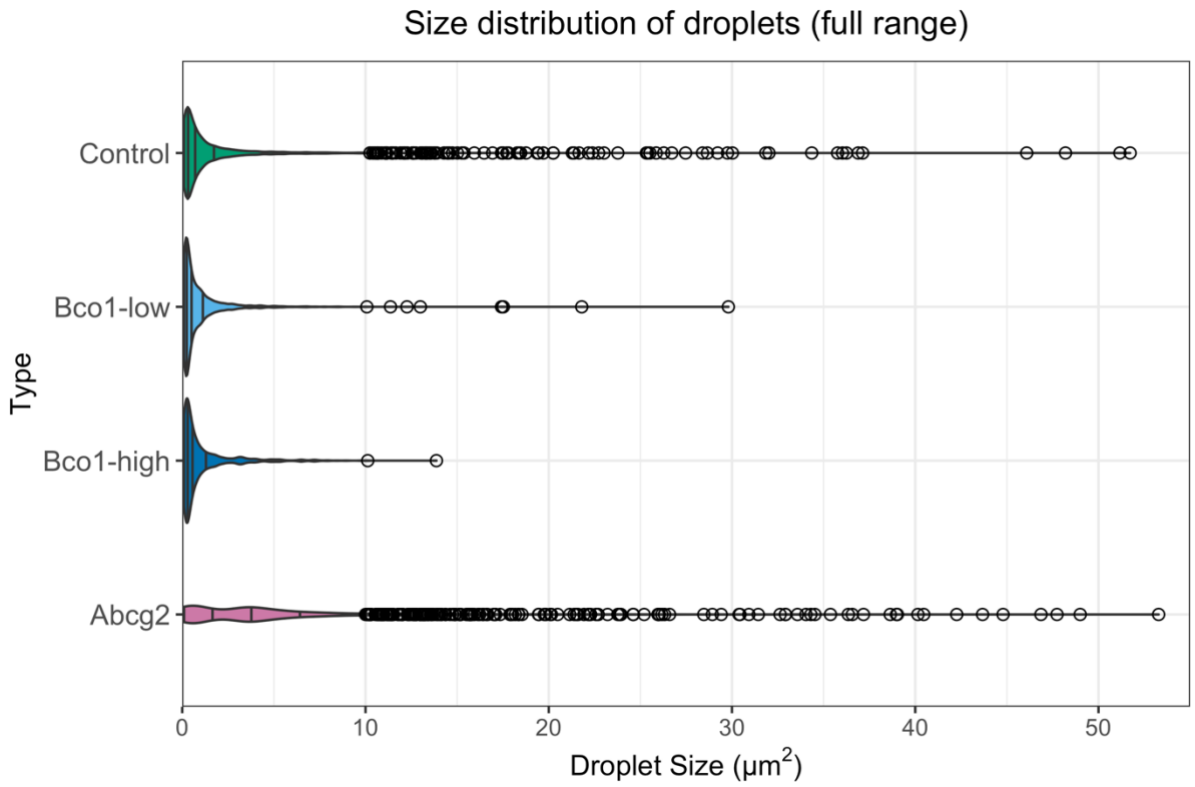

Figure 9: Full range droplet size distribution of liver samples. Circles represent droplets over 10μm². A bimodal curve is observed for abcg2 type. It looks slightly different from the bimodal curve observed in the Bco1-high intestine.

For the range of droplet size in the liver ranging from 0-11μm² (Figure 10), we can see the distribution between the KO´s median droplets are still significantly different from the control (*abcg2*^{KO}*:* 3.24 μm², *bco1*^{KO}-high 0.46 μm², *bco1*^{KO}-low 0.44 μm², control 0.63 μm²) (Wilcoxon pairwise t-test < 1.4e-07 (Supplemental Table 8)). It is observed that the *bco1*^{KO}-high and the *bco1*^{KO}-low types have very similar medians and were not significantly different from each other (Wilcoxon pairwise t-test = 0.13).

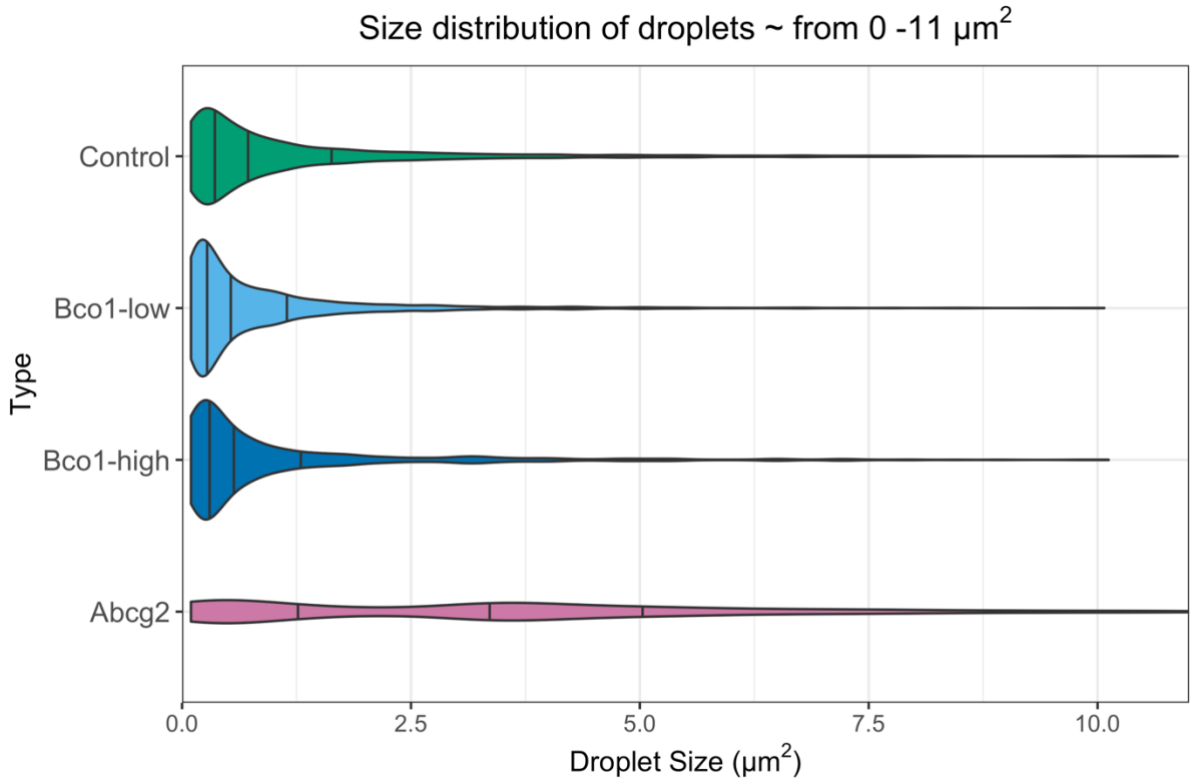

Figure 10: Droplet size distribution for droplets smaller than the cutoff value of 11 µm^2 for the liver. This zoomed-in distribution allows for closer examination of the different groups.

3.5 Differential expression of genes

RNA sequencing and differential gene expression (DEG) analysis was performed on the intestine and liver samples of the KO, control, and red and pale lines.

Starting with the most notable findings, *abcg2*^{KO} intestine was detected to have 1726 total genes showing to have differential expression. 262 DEG were upregulated (logFC > 1.0) and 75 (logFC < -1.0) were downregulated. Figure 11 shows the complete clustering network in the mid intestine (generated by STRING). In the mid intestine, the most significate upregulated networks included cholesterol biosynthetic process, sterol biosynthetic process, and GTPase activity. However, cholesterol biosynthetic pathways were also documented as being downregulated, along with cellular components. There were four genes to be directly involved in carotenoid metabolism (logFold2 change 1.0-1.3; 1-*apoA1, carm1, jun and rdh12*).

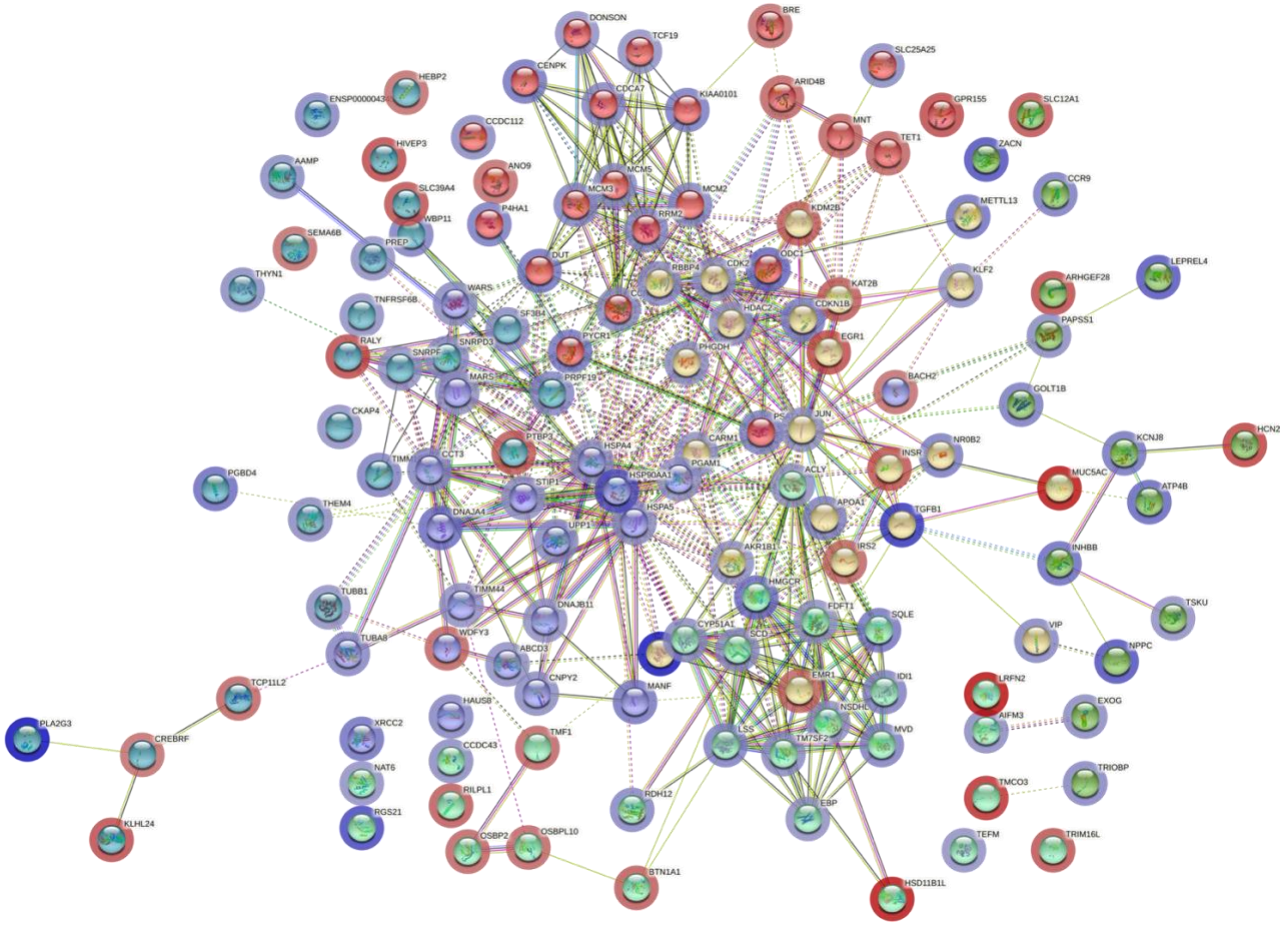

Figure 11: Complete cluster of the abcg2^{KO} intestine. Colored circles represent the individual gene. The colored outlines around the genes tell whether the gene is upregulated or downregulated with red meaning downregulated and blue meaning upregulated. The more intense the color, the stronger the up/downregulation.

When we take a closer look at the separated clusters, the most important is the cholesterol biosynthesis. Figure 12 shows the cholesterol related genes cluster. Here we can see that most of the gens involving cholesterol metabolism were upregulated. (GO:0006695) was the main GO term, which represents the cholesterol metabolism. Another major pathways that was upregulated was biosynthesis of steroids. Most of the genes involving cholesterol metabolism were upregulated, but there was a couple of genes that were downregulated that involved cholesterol metabolism.

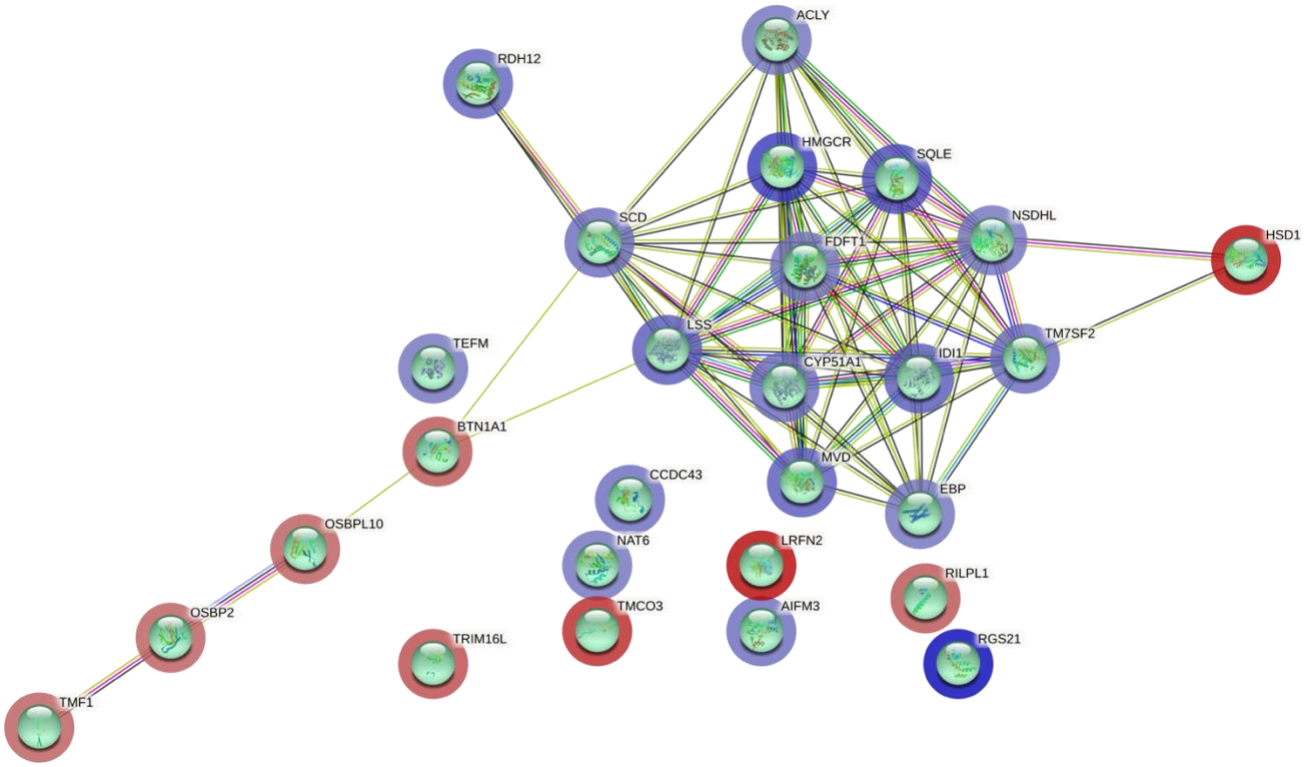

Figure 12: The cluster of cholesterol related genes. This is a small cluster from the whole network (from Figure 11). The colored outlines around the genes tell whether the gene is upregulated or downregulated with red meaning downregulated and blue meaning upregulated. The more intense the color, the strong the up/downregulation.

In the liver of *abcg2*^{KO} fish, many downregulated genes involved vitamin D synthesis such as positive regulation vitamin D 24-hydroxylase activity, vitamin D3 metabolic process, vitamin D3 metabolic process and positive regulation of cholesterol efflux.

There was no distinct differences *bco1*^{KO} high and low fish. However, in *bco1*^{KO} liver, 258 genes were differentially expressed (Figure 13). Upregulation of lipid metabolism was found (GO:0019216). Downregulation of positive regulation of cellular process were detected as well as genes involving response to hypoxia. Hypoxia was also found to be upregulated as well.

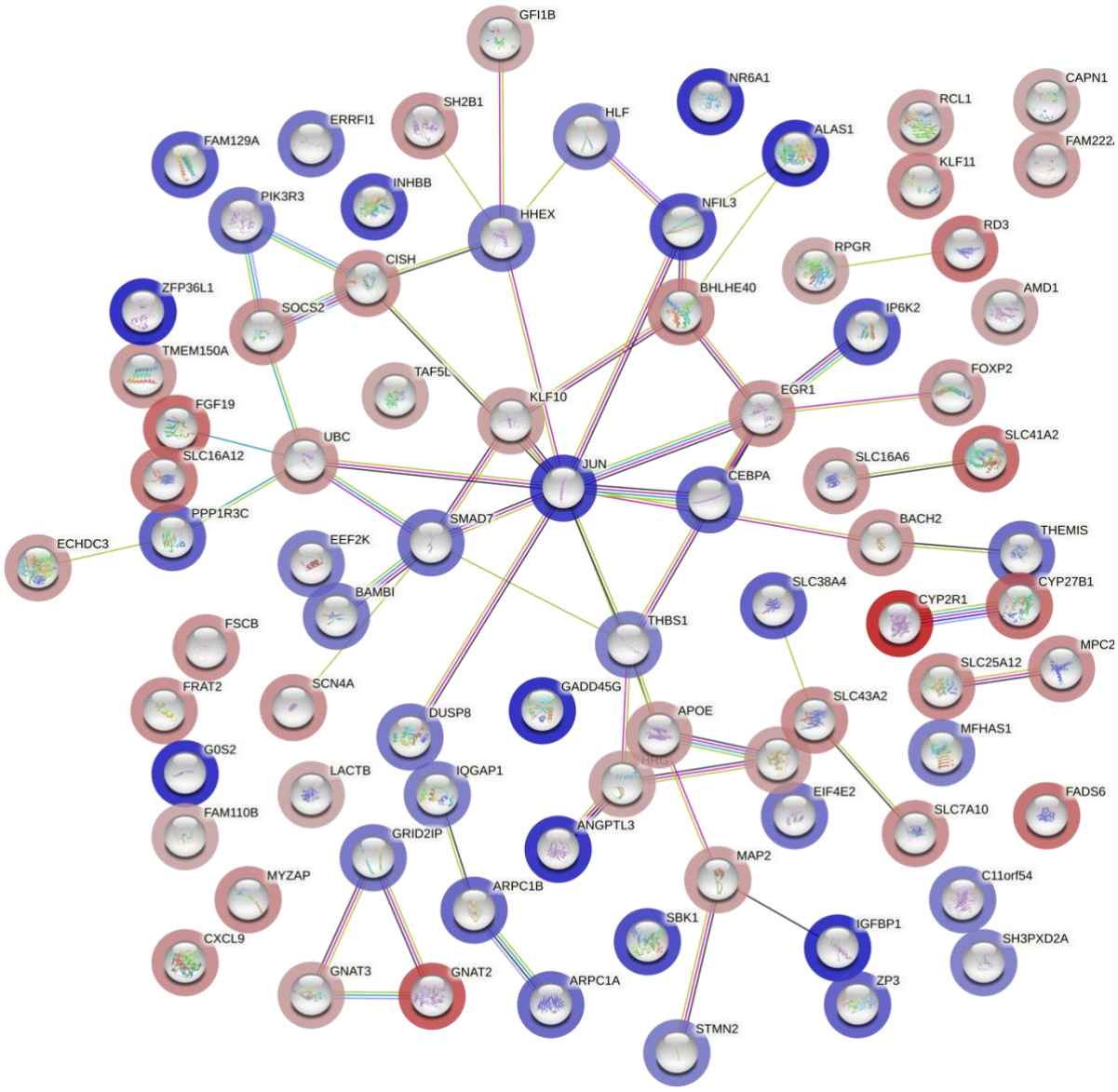

Figure 13: Cluster of bco1^{KO} liver. The colored outlines around the genes tell whether the gene is upregulated or downregulated with red meaning downregulated and blue meaning upregulated. The more intense the color, the strong the up/downregulation.

There was a lack of noteworthy genes identified in *bco1-like*^{KO}. However, in the liver there was CYP27B1 (25-hydroxyvitamin D-1 alpha hydroxylase) (GO:0010980) that was downregulated. Between the red and pale fish, the only analysis that showed they were genetically different was in the liver (55 DEG), but there were no significantly enriched genes that had a significance on color.

4 Discussion

This study aimed to observe the phenotypic effects of knocking out (KO) genes that previously have been linked to salmon muscle pigmentation by GWAS-studies (Baranski et al., 2010; Zoric, 2017). These genes included *abcg2*, *bco1* and *bco1-like*. This study looked at the impact the KO genes had on color, lipid accumulation, and droplet size.

The median a* mean value for the *bco1-like*^{KO} was the highest value of 6.36, and significantly higher than the control (Wilcoxon pairwise t-test < $2e^{-16}$), while the *bco1* gene showed the lowest value (5.08) among the KOs and it was not significantly different from the control (Wilcoxon pairwise t-test =0.96). These results suggest that the *bco1-like* enzyme is more active in degrading astaxanthin, compared to *bco1* enzyme. This result is also supported by the paper of Helgeland et al., (2019), which also concludes that *bco1-like* enzyme is more likely to influence astaxanthin degradation, compared to *bco1*. Since the *bco1* and *bco1-like* genes are located next to each other on salmon chromosome 26, it has not been possible to determine which one of the two genes regulates astaxanthin based on the GWAS-results alone.

The median a* mean value for the *abcg2*^{KO} had the second-highest value of 5.38 and was also significantly different from the control, indicating that also the *abcg2* transporter regulates astaxanthin. This is in line with the GWAS results (Zoric, 2017) and is also supported by a previous study of KOs by Wagnerberger (2020). In Wagnerberger (2020), the *abcg2*^{KO} effects were measured in Atlantic salmon four months after start-feeding. Wagnerberger (2020) found that the KO fish had double the amount of lipids in the intestine compared to the control, indicating that *abcg2* played an important role in exporting lipids from the enterocyte to the intestine, leading to lower astaxanthin levels. In this study, the same line of fish sampled after 11 months showed less of a difference between the KO groups and the control. The lipid content was higher in intestine of the KO groups compared to the control, but the difference was more distinguished in the fish sampled at four months.

As seen in Figure 6 A, the *abcg2*^{KO} had the highest median value of lipid area coverage in the intestine. It also had the highest median value for the number of droplets (Figure 6 B). *Bco1*^{KO} in both the high and low groups showed an increase in lipid area coverage and number of droplets. These results indicate that the *abcg2*^{KO} and the *bco1*^{KO} had increased lipid content in the intestine cells. This increased lipid content caused larger droplets to form. Looking at Figure 7, we see that there were many droplets in the *abcg2*^{KO} and *bco1*^{KO}-high that were larger

than 10 µm^2. However, in the *bco1*^{KO}-low, even though it had more lipid coverage area than the control, only < 1% of its droplets were above 10 µm^2. The control had a higher percentage of larger droplets above 10µm^2 when compared to the *bco1*^{KO}-low. We can then ask if droplet size had an impact on pigmentation since *bco1*^{KO}-high had a higher a* mean value and larger droplets compared to *bco1*^{KO}-low, which had a lower a* mean value and smaller droplets. Based on those results alone, it appears that there is a correlation between droplet size and pigmentation. However, when we look at the density graph (Figure 7), we can see the bimodal curve in the *bco1*^{KO}-high. This implies that there were some samples in the *bco1*^{KO}-high that had similar properties to the *bco1*^{KO}-low. Although *bco1*^{KO}-high and *bco1*^{KO}-low had similar sized droplets, *bco1*^{KO}-high had higher a* mean median values. This indicates that droplet size alone does not equate to higher red pigmentation. We also see that larger droplet size is not correlated to pigmentation when we compare the *bco1*^{KO}-high droplet size and a* mean value to the *abcg2*^{KO} droplet size and a* mean value. The *abcg2*^{KO} had smaller droplets compared to the *bco1*^{KO}-high, but it also had higher a* mean values which support the claim that droplet size is not related to redder fillet color in this study.

The lipid accumulation in the liver was highest in the *abcg2*^{KO} and was the only KO group to be different from the control (Figure 6 C). However, the *abcg2*^{KO} did not have the highest median value of droplets in the liver and was not significantly different from the control nor *bco1*^{KO}-high (Figure 6 D, Supplemental Table 3). The area covered by lipid in the *bco1*^{KO}-high and *bco1*^{KO}-low were not significantly different from each other nor the control (Supplemental Table 3). *Abcg2* may have a role with lipid transport in the liver, but the evidence shows it has a greater impact in the intestine. The droplet size in the *abcg2*^{KO} liver showed to have the largest median for droplet size at 3.46, but the control was the second highest in the group at 0.63 (Supplemental Table 7). Looking at the density curve in Figure 9, we can see that the *abcg2*^{KO} and the control had several droplet sizes above 10 µm^2 whereas the *bco1* groups only had a few in that range.

4.1 Knockout efficiencies

The main technique for determining the KO efficiency in this study was the modified getPCR method developed by Li et al. (2019). This procedure allows for comparison between the different KO groups. It was predicted that the higher the KO efficiency percentage, the higher the red pigmentation for the genes tested in this study. This is because these genes have the potential to either degrade pigment (*bco1* or *bco1-like*), or to transport pigment out of the cells

(*abcg2*). However, this is not what was observed (e.g., Figure 5). *Bco1*^{KO}-high had no correlation (slope = 0.003, p = 0.82, (Figure 5)) between KO efficiency and a* mean values, The same was also observed for *bco1-like*^{KO}. The KO efficiency values for the *bco1-like*^{KO} ranged from 71-100%, but the a* mean values did not increase as the KO efficiency increased (estimated slope = 0, p = 1.0 (Figure 5)). At 71%, the a* mean value was 9.03 whilst at 100% the a* mean values were ranging from 8.13-10.73. The *abcg2*^{KO} showed a negative correlation between KO efficiency and a* mean values (slope = -0.04, p = 0.13 (Figure 5)). It is worth noting the *bco1*^{KO}-low values where the slope was negative as well as showing a clear relationship between KO efficiency and color (p = 0.004). This means that the higher the KO efficiency was, the less intense the color was.

Although we expected a positive correlation between the KO efficiency and a* mean values for *abcg2*^{KO} *bco1*^{KO}, and *bco1-like*^{KO}, this was not documented in this study. A possible reason for this could be because the KO efficiency estimates from the getPCR does not accurately estimate the relative amount of CRISPR-edited cells in each individual. The getPCR is based on small tissue samples where the relative amounts of CRISPR-edited vs wild type cells are estimated. These small tissue samples are not necessarily representative of the whole fish. Theoretically, one additional reason for the unexpected results could be that the threshold for KO-efficiency to be sufficient for flesh pigmentation is smaller than what is observed and that only a small KO efficiency percentage is needed to achieve observable effects on pigmentation. However, it seems unlikely that, e.g., an *abcg2*^{KO}, efficiency below 40% is sufficient to obtain maximum phenotypic effect caused by this gene.

4.2 Relationship between astaxanthin and lipids

It could not be confirmed if increased lipid content leads to increased astaxanthin levels. While this study did use the Minolta reader to test the intensity of the red color of the fillet, there was no experiment to determine the amount of astaxanthin in the flesh. The amount of astaxanthin could be measured by using microscopy by using certain stains that would allow the astaxanthin molecule to be detected. Furthermore, it was undetermined if the gene KO types had a huge effect on pigmentation. While in some cases, the gene KO types did show an increase in lipids, it is unknown if the lipid content improved astaxanthin uptake in the flesh.

The *abcg2* gene is a transporter for lipids. It impacts the pigmentation of salmon fillet because it exports astaxanthin from the enterocytes back out into the lumen where it leaves the body. It

is predicted that if this gene is knocked out, then the transportation of lipids of astaxanthin out of the body would be halted. The *abcg2*^{KO} samples showed an increase lipid content in the intestine, showing that the *abcg2* is linked to lipid transport. The droplet sizes in the *abcg2*^{KO} were on average larger than the control. The larger droplets are most likely formed from the accumulation of smaller droplets on the intestinal wall. Since the droplets are not getting transported, the droplets fuse together with each other, creating larger droplets. This reasoning also explains why the lipid area coverage between the groups were not significantly different whereas they all ranged in droplet sizes. One big droplet was about equal size to several droplets in terms of lipid area. The increased lipid content only caused large droplets to form in the *abcg2* and the *bco1*. But this larger amount of droplets does not prove if *abcg2* or *bco1* is involved in the increased amount of lipids in the intestine cells.

Bco1/bco1-like are cytosol enzymes that degrade astaxanthin. These enzymes are found in the same location as each other on ssa26 and are known to degrade carotenoids. With these genes knocked out, then less degradation of astaxanthin would occur, meaning more pigment can accumulate in the flesh. The *bco1*^{KO} had the widest range of a* mean values where some values were below the lowest a* mean values of the control type (Figure 4). The *bco1*^{KO} was then split up to compare the samples that had mean values lower than the control group against the ones that had higher a* mean values (*bco1*^{KO}-low vs *bco1*^{KO}-high). Interestingly, there were no significant differences in lipid area coverage and number of droplets between the two *bco1*^{KO} in both intestine and liver. *Bco1*^{KO}-high, however, had the largest median droplet size in the intestine at 3.97 μm^2 compared to the *bco1*^{KO}-low type at 0.46 μm^2 (Supplemental Table 5). This was the only category where the *bco1*^{KO}-high type and the *bco1*^{KO}-low type were significantly different (Wilcoxon pairwise t-test < 2e-16). The split in the *bco1*^{KO} type shows that the KO efficiency in *bco1* is not that effective. If there was a true distinction between the *bco1*^{KO}-high and the *bco1*^{KO}-low groups other than a* mean value color, then there should have been more differences in the intestine and liver.

The *bco1-like*^{KO} had the highest KO efficiency as well as the highest color in the fillet (a* mean value of 6.36). This could mean that knocking out the *bco1-like*^{KO} had a greater impact on astaxanthin. Due to the lack of the *bco1-like*^{KO} samples, microscopy was not performed on the *bco1-like*^{KO} samples, so lipid accumulation in the intestine and liver is unknown. Since neither the *abcg2*^{KO} nor the *bco1*^{KO} types had high a* mean values, it is difficult to predict what the lipid accumulation would have looked like for samples with high a* mean values. However,

the a* mean values were gathered as well as the KO efficiencies so some conclusions can still be made based on those pieces of data. Based on the a* mean values, the *bco1-like*^{KO} had higher values than the *bco1*^{KO}. This supports that the *bco1-like*^{KO} is more relevant when it comes to flesh pigmentation when compared to the *bco1*^{KO}. This study did show that the *bco1-like* does have a role in flesh pigmentation since the *bco1-like*^{KO} samples had an increase in red pigmentation. The only evidence of this was based on the a* mean value figure (Figure 4), where *bco1-like*^{KO} was the reddest compared to the other knockout groups. It might be of interest in future studies to figure out the concentration of astaxanthin in the fish and compare those numbers with each other. It is reasonable to assume that the *bco1-like*^{KO} had the most astaxanthin in the flesh based on the Minolta readings.

4.3 Differentially expressed genes

The number of DEG ($p < 0.5$) varies between the different KO lines. The most enriched pathways involving lipid metabolism were detected in the *abcg2*^{KO} intestine and the *bco1*^{KO} liver. Those two will be the main focus for the rest of differentially expressed genes. The other genes found in *abcg2*^{KO} liver, *bco1*^{KO} intestine, *bco1-like*^{KO} and red versus pale showed to have no significant impact on lipid metabolism and thereby won´t be mentioned further.

In the *abcg2*^{KO} intestine, the main finding involved cholesterol metabolism. This was of interest because it directly involved with lipid transport. *Abcg2* is known in mammals to transport lipids and has a role in regulating cholesterol transport (Kerr et al., 2021). With the *abcg2* being knocked out, less expression of lipid transport is predicted to be seen, leading to increased amounts of lipids in the intestine villi. In the *abcg2*^{KO} intestine differentially expressed genes, we see an increase of cholesterol metabolism where Figure 12 shows the cluster chart in cholesterol metabolism. Figure 12 shows the relationship between the cholesterol genes that are found in *abcg2*^{KO} intestine. There were several genes that were upregulated and having an impact that was significant. *Abcg2*^{KO} intestine had the most impact on lipid metabolism and had the most dramatic effect on gene expression. This data shows that salmon are impacted by *abcg2´*s effect on cholesterol metabolism in a similar way that is documented in mammals. Genes that were found in the *abcg2*^{KO} intestine that are involved carotenoid metabolism are *ApoA1*, *Carm1*, *JUN*, and *RDH12*. In addition, there were several downregulated genes involving vitamin D synthesis. Overall, the *abcg2*^{KO} in the intestine appeared to have an impact on lipid metabolism. This is supported by the fact that Figure 6 showed that the *abcg2*^{KO} had increased lipid accumulation compared to the control.

There was no distinction between *bco1*^{KO}-low and *bco1*^{KO}-high. This was unexpected because it was predicted that there should have been some genes that might have explained the differences between the low and high *bco1*^{KO}. Looking at just *bco1*^{KO} liver, there were several significantly enriched genes which the most notable one being the upregulated of lipid metabolic processes. *Bco1* could play a role in upholding normal hepatic lipid and cholesterol homeostasis (Lim et al., 2018). By knocking out the *bco1*, there was some increased lipid accumulation (Figure 6) suggesting that *bco1* does play a role in lipid metabolism.

5 Conclusion

The purpose of this paper was to achieve a better understanding of the effect of knocking out genes that have been related to muscle pigmentation in previous GWAS-studies. The targeted genes included *abcg2*, *bco1*, and *bco1-like* and they were knocked out by the gene editing technique CRISPR/CAS9.

To test if the gene knockouts had increased red color, a Minolta colorimeter was used to detect the a* intensity (red color). There it was observed amongst the KO groups and control that *bco1-like*^{KO} had the highest red pigmentation. *Abcg2*^{KO} had the second highest a* mean value, and the *bco1*^{KO} had similar pigmentation to the control. GetPCR was used to determine the KO efficiency where the sample fish were matched with their respected a* mean values. There was no clear correlation between having a high KO efficiency and high red color. Microscopy was used to observe the amount of lipids in the knockout fish where the *abcg2*^{KO} had the most lipid accumulation of all the groups. Differential gene analysis was used to take a deeper look into the genes and see if any were related to lipid metabolism. The *abcg2*^{KO} intestine showed that there were some pathways involving cholesterol metabolism. Furthermore, the *abcg2* gene played an important role in lipid transportation. In previous GWAS studies, it is known *abcg2* has an impact on flesh pigmentation because of its ability to export lipids and astaxanthin from the enterocyte to the intestinal lumen. *Bco1-like* was also predicted to have an impact on flesh pigmentation because of its ability to degrade astaxanthin. In this study, *bco1-like*^{KO} fish had the greatest red color compared to the other KO groups and the control. However, more research is needed to flesh out the details of the exact impact *bco1-like* has on lipid metabolism.

6 Citations

Aas, T. S., Ytrestøyl, T. & Åsgård, T. (2019). Utilization of feed resources in the production of Atlantic salmon (Salmo salar) in Norway: An update for 2016. *Aquaculture Reports*, 15: 100216.

Ando, S., Takeyama, T., Hatano, M. & Zama, K. (1985). Carotenoid-carrying lipoproteins in the serum of chum salmon (Oncorhynchus keta) associated with migration. *Agricultural and biological chemistry*, 49 (7): 2185-2187.

Arganda-Carreras, I., Kaynig, V., Rueden, C., Eliceiri, K. W., Schindelin, J., Cardona, A. & Sebastian Seung, H. (2017). Trainable Weka Segmentation: a machine learning tool for microscopy pixel classification. *Bioinformatics*, 33 (15): 2424-2426. doi: 10.1093/bioinformatics/btx180.

Baranski, M., Moen, T. & Våge, D. I. (2010). Mapping of quantitative trait loci for flesh colour and growth traits in Atlantic salmon (Salmo salar). *Genetics Selection Evolution*, 42 (1): 1-14.

Bell, J. G., McEvoy, J., Tocher, D. R. & Sargent, J. R. (2000). Depletion of α-tocopherol and astaxanthin in Atlantic salmon (Salmo salar) affects autoxidative defense and fatty acid metabolism. *The Journal of nutrition*, 130 (7): 1800-1808.

Bjerkeng, B., Storebakken, T. & Liaaen-Jensen, S. (1992). Pigmentation of rainbow trout from start feeding to sexual maturation. *Aquaculture*, 108 (3-4): 333-346.

Bjerkeng, B. & Berge, G. (2000). Apparent digestibility coefficients and accumulation of astaxanthin E/Z isomers in Atlantic salmon (Salmo salar L.) and Atlantic halibut (Hippoglossus hippoglossus L.). *Comparative Biochemistry and Physiology Part B: Biochemistry and Molecular Biology*, 127 (3): 423-432.

Borel, P., Grolier, P., Armand, M., Partier, A., Lafont, H., Lairon, D. & Azaïs-Braesco, V. (1996). Carotenoids in biological emulsions: solubility, surface-to-core distribution, and release from lipid droplets. *Journal of lipid research*, 37 (2): 250-261.

Christiansen, R., Lie, O. & Torrissen, O. (1995). Growth and survival of Atlantic salmon, Salmo salar L., fed different dietary levels of astaxanthin. First-feeding fry. *Aquaculture Nutrition*, 1 (3): 189-198.

Clark, R. M., Yao, L., She, L. & Furr, H. C. (2000). A comparison of lycopene and astaxanthin absorption from corn oil and olive oil emulsions. *Lipids*, 35 (7): 803-806.

Clevidence, B. A. & Bieri, J. G. (1993). [4] Association of carotenoids with human plasma lipoproteins. In vol. 214 *Methods in enzymology*, pp. 33-46: Elsevier.

Dean, M. & Allikmets, R. (1995). Evolution of ATP-binding cassette transporter genes. *Current opinion in genetics & development*, 5 (6): 779-785.

FAO. (2020). *The State of World Fisheries and Aquaculture 2020. Sustainability in Action*. Rome.

Gjedrem, T., Robinson, N. & Rye, M. (2012). The importance of selective breeding in aquaculture to meet future demands for animal protein: a review. *Aquaculture*, 350: 117-129.

Goodwin, T. (1980). Nature and distribution of carotenoids. *Food Chemistry*, 5 (1): 3-13.

Gottesman, M. M., Fojo, T. & Bates, S. E. (2002). Multidrug resistance in cancer: role of ATP–dependent transporters. *Nature reviews cancer*, 2 (1): 48-58.

Helgeland, H., Sodeland, M., Zoric, N., Torgersen, J. S., Grammes, F., von Lintig, J., Moen, T., Kjøglum, S., Lien, S. & Våge, D. I. (2019). Genomic and functional gene studies suggest a key role of beta-carotene oxygenase 1 like (bco1l) gene in salmon flesh color. *Scientific reports*, 9 (1): 1-12.

Houston, R. D., Taggart, J. B., Cézard, T., Bekaert, M., Lowe, N. R., Downing, A., Talbot, R., Bishop, S. C., Archibald, A. L. & Bron, J. E. (2014). Development and validation of a high density SNP genotyping array for Atlantic salmon (Salmo salar). *BMC genomics*, 15 (1): 1-13.

Jacobsen, J. A. & Hansen, L. P. (2001). Feeding habits of wild and escaped farmed Atlantic salmon, Salmo salar L., in the Northeast Atlantic. *ICES Journal of Marine Science*, 58 (4): 916-933.

Kerr, I. D., Hutchison, E., Gerard, L., Aleidi, S. M. & Gelissen, I. C. (2021). Mammalian ABCG-transporters, sterols and lipids: To bind perchance to transport? *Biochimica et Biophysica Acta (BBA)-Molecular and Cell Biology of Lipids*, 1866 (3): 158860.

Kidd, P. (2011). Astaxanthin, cell membrane nutrient with diverse clinical benefits and anti-aging potential. *Altern Med Rev*, 16 (4): 355-364.

Li, B., Ren, N., Yang, L., Liu, J. & Huang, Q. (2019). A qPCR method for genome editing efficiency determination and single-cell clone screening in human cells. *Scientific reports*, 9 (1): 1-15.

Lim, J. Y., Liu, C., Hu, K.-Q., Smith, D. E. & Wang, X.-D. (2018). Ablation of carotenoid cleavage enzymes (BCO1 and BCO2) induced hepatic steatosis by altering the farnesoid X receptor/miR-34a/sirtuin 1 pathway. *Archives of Biochemistry and Biophysics*, 654: 1-9. doi: https://doi.org/10.1016/j.abb.2018.07.007.

Liu, Y., Olaf Olaussen, J. & Skonhoft, A. (2011). Wild and farmed salmon in Norway—A review. *Marine Policy*, 35 (3): 413-418. doi: https://doi.org/10.1016/j.marpol.2010.11.007.

Lorenz, R. T. & Cysewski, G. R. (2000). Commercial potential for Haematococcus microalgae as a natural source of astaxanthin. *Trends in biotechnology*, 18 (4): 160-167.

Matthews, S. J., Ross, N. W., Lall, S. P. & Gill, T. A. (2006). Astaxanthin binding protein in Atlantic salmon. *Comparative Biochemistry and Physiology Part B: Biochemistry and Molecular Biology*, 144 (2): 206-214.

Miki, W. (1991). Biological functions and activities of animal carotenoids. *Pure and applied chemistry*, 63 (1): 141-146.

Naguib, Y. M. (2000). Antioxidant activities of astaxanthin and related carotenoids. *Journal of agricultural and food chemistry*, 48 (4): 1150-1154.

Norwegian Seafood Council. (2022). *Nøkkeltall*. Available at: https://nokkeltall.seafood.no/ (accessed: 13.04.2022).

Page, G. & Davies, S. (2003). Hepatic carotenoid uptake in rainbow trout (Oncorhynchus mykiss) using an isolated organ perfusion model. *Aquaculture*, 225 (1-4): 405-419.

Quinton, C. D., McMillan, I. & Glebe, B. D. (2005). Development of an Atlantic salmon (Salmo salar) genetic improvement program: Genetic parameters of harvest body weight and carcass quality traits estimated with animal models. *Aquaculture*, 247 (1-4): 211-217.

Raghuvanshi, S., Reed, V., Blaner, W. S. & Harrison, E. H. (2015). Cellular localization of β-carotene 15, 15′ oxygenase-1 (BCO1) and β-carotene 9′, 10′ oxygenase-2 (BCO2) in rat liver and intestine. *Archives of biochemistry and biophysics*, 572: 19-27.

Ranga Rao, A., Raghunath Reddy, R., Baskaran, V., Sarada, R. & Ravishankar, G. (2010). Characterization of microalgal carotenoids by mass spectrometry and their bioavailability and antioxidant properties elucidated in rat model. *Journal of agricultural and food chemistry*, 58 (15): 8553-8559.

Sarkadi, B., Özvegy-Laczka, C., Német, K. & Váradi, A. (2004). ABCG2–a transporter for all seasons. *FEBS letters*, 567 (1): 116-120.

Schiedt, K., Leuenberger, F., Vecchi, M. & Glinz, E. (1985). Absorption, retention and metabolic transformations of carotenoids in rainbow trout, salmon and chicken. *Pure and Applied Chemistry*, 57 (5): 685-692.

Schindelin, J., Arganda-Carreras, I., Frise, E., Kaynig, V., Longair, M., Pietzsch, T., Preibisch, S., Rueden, C., Saalfeld, S., Schmid, B., et al. (2012). Fiji: an open-source platform for biological-image analysis. *Nature Methods*, 9 (7): 676-682. doi: 10.1038/nmeth.2019.

Sissener, N., Torstensen, B. E., Ruyter, B., Torstensen, B. E., Ruyter, B., Østbye, T.-K., Waagbø, R., Jørgensen, S. M., Hatlen, B., Liland, N., et al. (2016). *Oppdatering av utredningen: Effekter av endret fettsyresammensetning i fôr til laks relatert til fiskens helse, velferd og robusthet*: Nofima.

Statistics Norway. (2020). *Aquaculture (terminated in Statistics Norway)*. Available at: https://www.ssb.no/en/fiskeoppdrett?fbclid=IwAR3tfBgKLDC8dXSxLa7fgVw92unMSweQxH6n3lmi27WJbRqOBzlQlN-8SFA (accessed: 16.02.2022).

Steven, D. (1948). Studies on animal carotenoids: I. Carotenoids of the brown trout (Salmo trutta linn.). *Journal of experimental Biology*, 25 (4): 369-387.

Storebakken, T. & No, H. K. (1992). Pigmentation of rainbow trout. *Aquaculture*, 100 (1-3): 209-229.

Szklarczyk, D., Gable, A. L., Nastou, K. C., Lyon, D., Kirsch, R., Pyysalo, S., Doncheva, N. T., Legeay, M., Fang, T. & Bork, P. (2021). The STRING database in 2021: customizable

protein–protein networks, and functional characterization of user-uploaded gene/measurement sets. *Nucleic acids research*, 49 (D1): D605-D612.

Thompson, I., Choubert, G., Houlihan, D. & Secombes, C. (1995). The effect of dietary vitamin A and astaxanthin on the immunocompetence of rainbow trout. *Aquaculture*, 133 (2): 91-102.

Torrissen, O., Hardy, R., Shearer, K., Scott, T. & Stone, F. (1990). Effects of dietary canthaxanthin level and lipid level on apparent digestibility coefficients for canthaxanthin in rainbow trout (Oncorhynchus mykiss). *Aquaculture*, 88 (3-4): 351-362.

Torrissen, O. J. (1989). Pigmentation of salmonids: interactions of astaxanthin and canthaxanthin on pigment deposition in rainbow trout. *Aquaculture*, 79 (1-4): 363-374.

Torstensen, B., Espe, M., Sanden, M., Stubhaug, I., Waagbø, R., Hemre, G.-I., Fontanillas, R., Nordgarden, U., Hevrøy, E. & Olsvik, P. (2008). Novel production of Atlantic salmon (Salmo salar) protein based on combined replacement of fish meal and fish oil with plant meal and vegetable oil blends. *Aquaculture*, 285 (1-4): 193-200.

Wagnerberger, J. H. (2020). *CRISPR based functional characterization of the abcg2b gene contribution to muscle pigmentation in Atlantic salmon*. Master thesis: Norwegian University of Life Sciences, Ås (accessed: 26.05.2021).

White, D., Ørnsrud, R. & Davies, S. (2003). Determination of carotenoid and vitamin A concentrations in everted salmonid intestine following exposure to solutions of carotenoid in vitro. *Comparative Biochemistry and Physiology Part A: Molecular & Integrative Physiology*, 136 (3): 683-692.

Ytrestøyl, T., Aas, T. S. & Åsgård, T. (2015). Utilisation of feed resources in production of Atlantic salmon (Salmo salar) in Norway. *Aquaculture*, 448: 365-374.

Zaripheh, S. & Erdman Jr, J. W. (2002). Factors that influence the bioavailablity of xanthophylls. *The Journal of nutrition*, 132 (3): 531S-534S.

Zoric, N. (2017). *Characterization of genes and gene products influencing carotenoid metabolism in Atlantic salmon*. Ph.D. thesis: Norwegian University of Life Sciences, Ås (accessed: November, 2021).

7 Appendix

Supplemental Table 1: KO and control (Type) in the intestine with median and IQR for lipid coverage percentage with test statistics for Pairwise comparisons using Wilcoxon rank-sum test with continuity correction (Benjamini & Hochberg, 1995). The count is the total number of samples in each.

Type	Count	Median (%)	IQR	Pairwise Wilcox Test			
Abcg2	61	1.67	2.60		Abcg2	Bco1-high	Bco1-low
Bco1-high	66	1.01	1.16	Bco1-high	0.08	-	-
Bco1-low	58	1.27	1.29	Bco1-low	0.11	0.76	-
Control	75	0.34	0.76	Control	1.3e-07	3.6e-06	2.1e-06

Supplemental Table 2: KO groups and control (Type) in the intestine with median and IQR for droplets per μm^2 with test statistics for Pairwise comparisons using Wilcoxon rank-sum test with continuity correction (Benjamini & Hochberg, 1995). The count is the total number of samples in each type.

Type	Count	Median	IQR	Pairwise Wilcox Test			
Abcg2	61	0.019	0.020		Abcg2	Bco1-high	Bco1-low
Bco1-high	66	0.014	0.012	Bco1-high	0.58	-	-
Bco1-low	58	0.016	0.021	Bco1-low	0.82	0.75	-
Control	75	0.0061	0.014	Control	8.9e-05	8.9e-05	7.9e-05

Supplemental Table 3: KO groups and control (Type) in the liver with median and IQR for lipid coverage percentage with test statistics for Pairwise comparisons using Wilcoxon rank-sum test with continuity correction (Benjamini & Hochberg, 1995). The count is the total number of samples in each type.

Type	Count	Median (%)	IQR	Pairwise Wilcox Test			
Abcg2	55	0.34	0.55		Abcg2	Bco1-high	Bco1-low
Bco1-high	32	0.22	0.25	Bco1-high	0.034	-	-
Bco1-low	25	0.32	0.36	Bco1-low	0.30	0.30	-
Control	78	0.18	0.66	Control	0.017	0.45	0.30

Supplemental Table 4: KO groups and control (Type) in the liver with median and IQR for droplets per μm^2 with test statistics for Pairwise comparisons using Wilcoxon rank sum test with continuity correction (Benjamini & Hochberg, 1995). Count is the total number of samples in each type.

Type	Count	Median	IQR	Pairwise Wilcox Test			
Abcg2	55	0.0025	0.0022		Abcg2	Bco1-high	Bco1-low
Bco1-high	32	0.0024	0.0023	Bco1-high	0.512	-	-
Bco1-low	25	0.0036	0.0028	Bco1-low	0.282	0.151	-
Control	78	0.0019	0.0027	Control	0.044	0.220	0.032

Supplemental Table 5: KO groups and control (Type) in the intestine with median droplet size (μm^2) and IQR values with test statistics for Pairwise comparisons using Wilcoxon rank sum test with continuity correction (Benjamini & Hochberg, 1995). Count is the total number of droplets in each.

Type	Count	Median	IQR	Pairwise Wilcox Test			
Abcg2	20117	0.51	0.80		Abcg2	Bco1-high	Bco1-low
Bco1-high	892	3.97	2.66	Bco1-high	<2e-16	-	-
Bco1-low	17324	0.46	0.63	Bco1-low	<2e-16	<2e-16	-
Control	5510	0.34	0.51	Control	<2e-16	<2e-16	<2e-16

Supplemental Table 6: KO and control (Type) of intestine with median droplet size (µm^2) and IQR values with the range of 0-11 µm2 with test statistics for Pairwise comparisons using Wilcoxon rank sum test with continuity correction (Benjamini & Hochberg, 1995).

Type	Count	Median	IQR	Pairwise Wilcox Test			
Abcg2	20035	0.51	0.80		Abcg2	Bco1-high	Bco1-low
Bco1-high	834	3.82	2.28	Bco1-high	<2e-16	-	-
Bco1-low	17316	0.46	0.63	Bco1-low	<2e-16	<2e-16	-
Control	5506	0.34	0.51	Control	<2e-16	<2e-16	<2e-16

Supplemental Table 7: KO groups and control (Type) in the liver with median droplet size (µm2) and IQR values with test statistics for Pairwise comparisons using Wilcoxon rank sum test with continuity correction (Benjamini & Hochberg, 1995). Count is the total number of droplets in each.

Type	Count	Median	IQR	Pairwise Wilcox Test			
Abcg2	1359	3.46	5.05		Abcg2	Bco1-high	Bco1-low
Bco1-high	961	0.46	0.10	Bco1-high	<2e-16	-	-
Bco1-low	2083	0.44	0.85	Bco1-low	<2e-16	0.16	-
Control	3602	0.63	1.36	Control	<2e-16	1.3 <-16	<2e-16

Supplemental Table 8: KO and control (Type) of liver with median droplet size (µm^2) and IQR values with the range of 0-11 µm2 with test statistics for Pairwise comparisons using Wilcoxon rank sum test with continuity correction (Benjamini & Hochberg, 1995).

Type	Count	Median	IQR	Pairwise Wilcox Test			
Abcg2	1208	3.24	4.09		Abcg2	Bco1-high	Bco1-low
Bco1-high	960	0.46	0.90	Bco1-high	<2e-16	-	-
Bco1-low	2076	0.44	0.83	Bco1-low	<2e-16	0.13	-
Control	3501	0.63	0.63	Control	<2e-16	<1.4e-07	<2e-16

Supplemental Table 9: Results from the a value means from the Minolta colorimeter*

Type	Count	Median	IQR	Pairwise Wilcox Test			
Abcg2	107	5.38	1.04		Abcg2	Bco1	Bco1-like
Bco1	173	5.08	1.45	Bco1	0.0079	-	-
Bco1-like	155	6.36	1.53	Bco1-like	6.8 e-14	<2e-16	-
Control	66	5.01	1.31	Control	0.02	0.96	2.4e-16

Supplemental Table 10: Commercial diet for the salmon

Type	Amount
Rapid 80	40 mg asta/kg
Rapid 200	40 mg asta/kg
Dermic 500	50 mg asta/kg
Rapid 1000	50 mg/kg

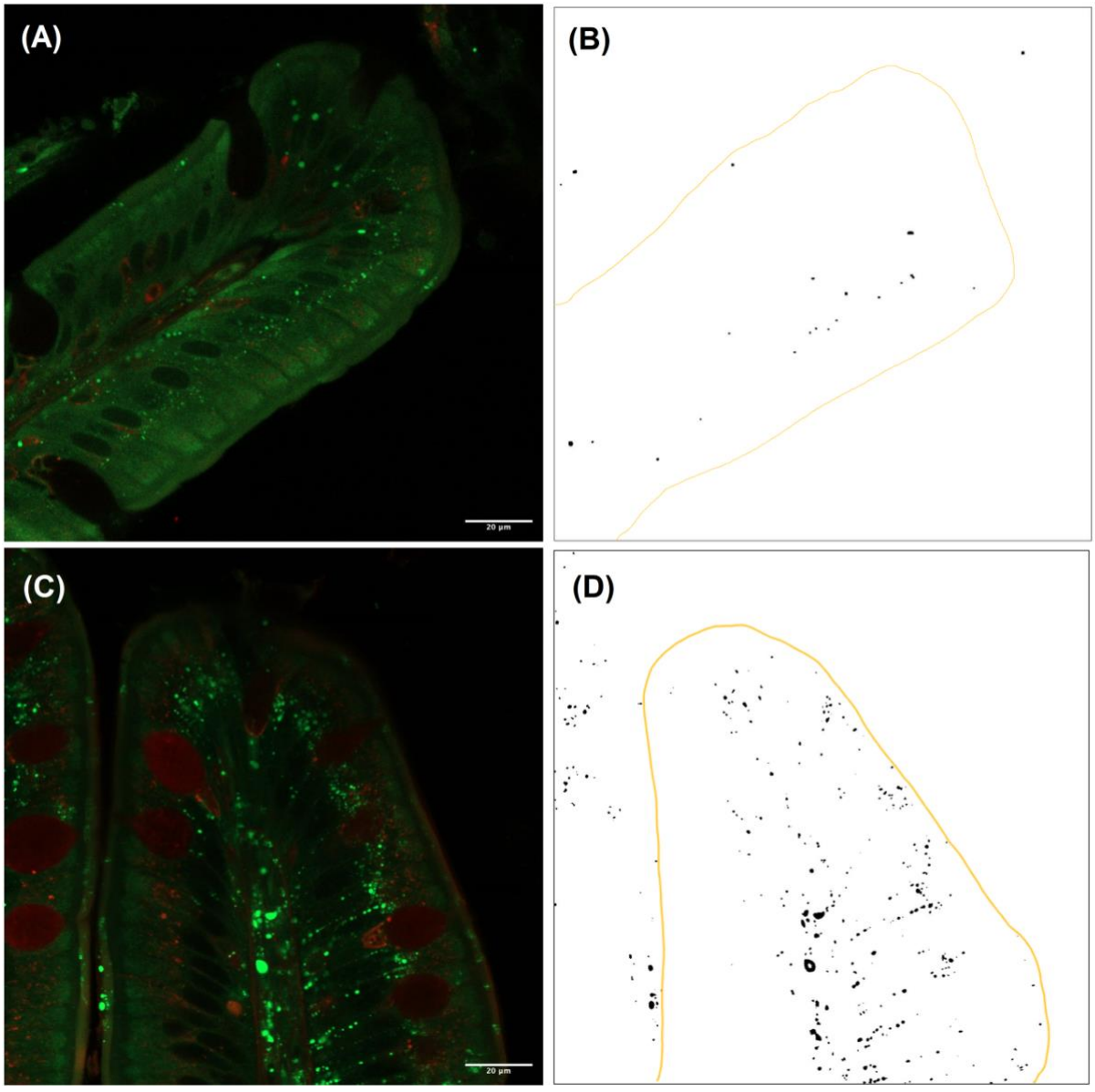

Figure 14: Control intestine

g

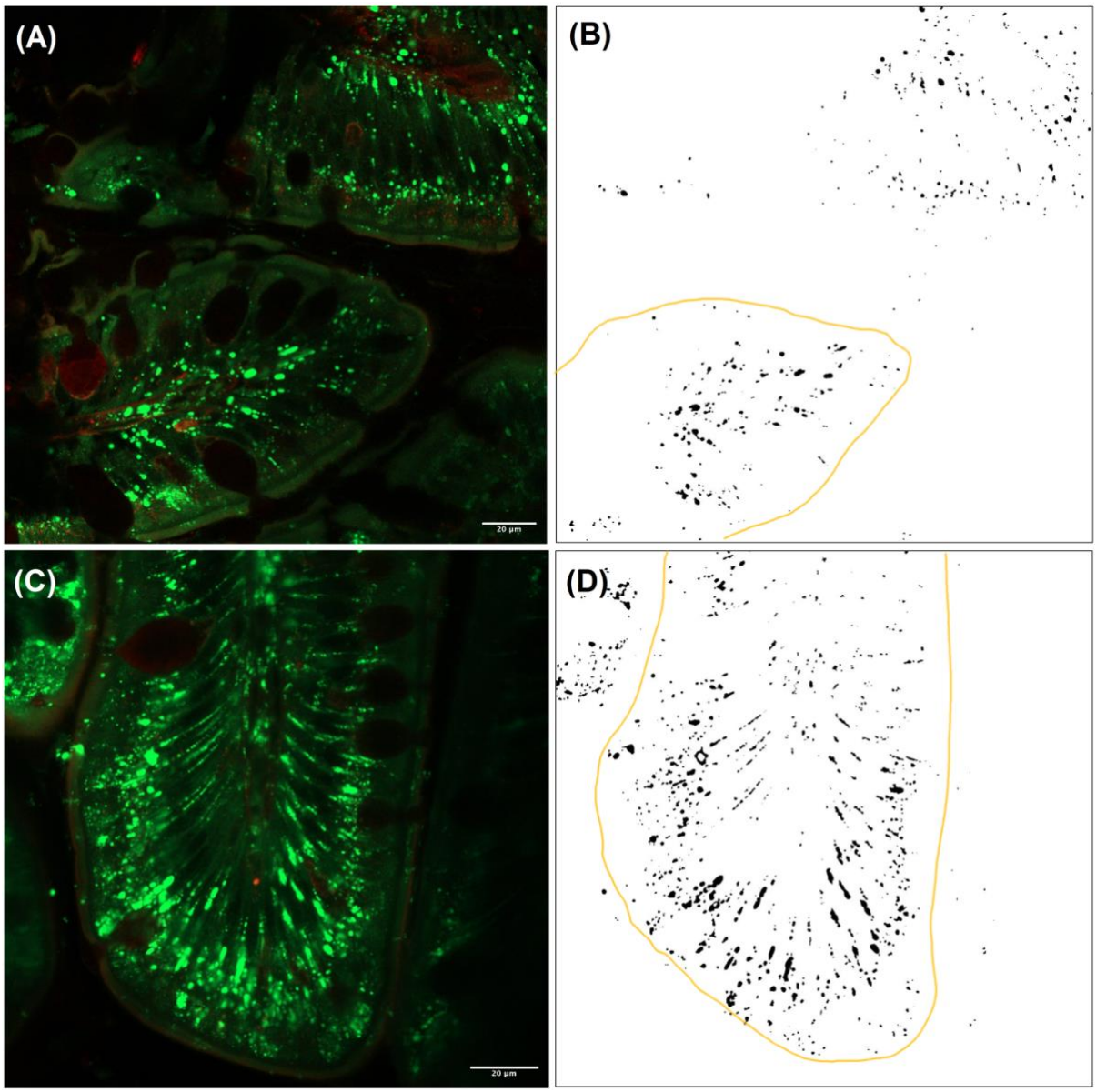

Figure 15: Abcg2^{KO} Intestine

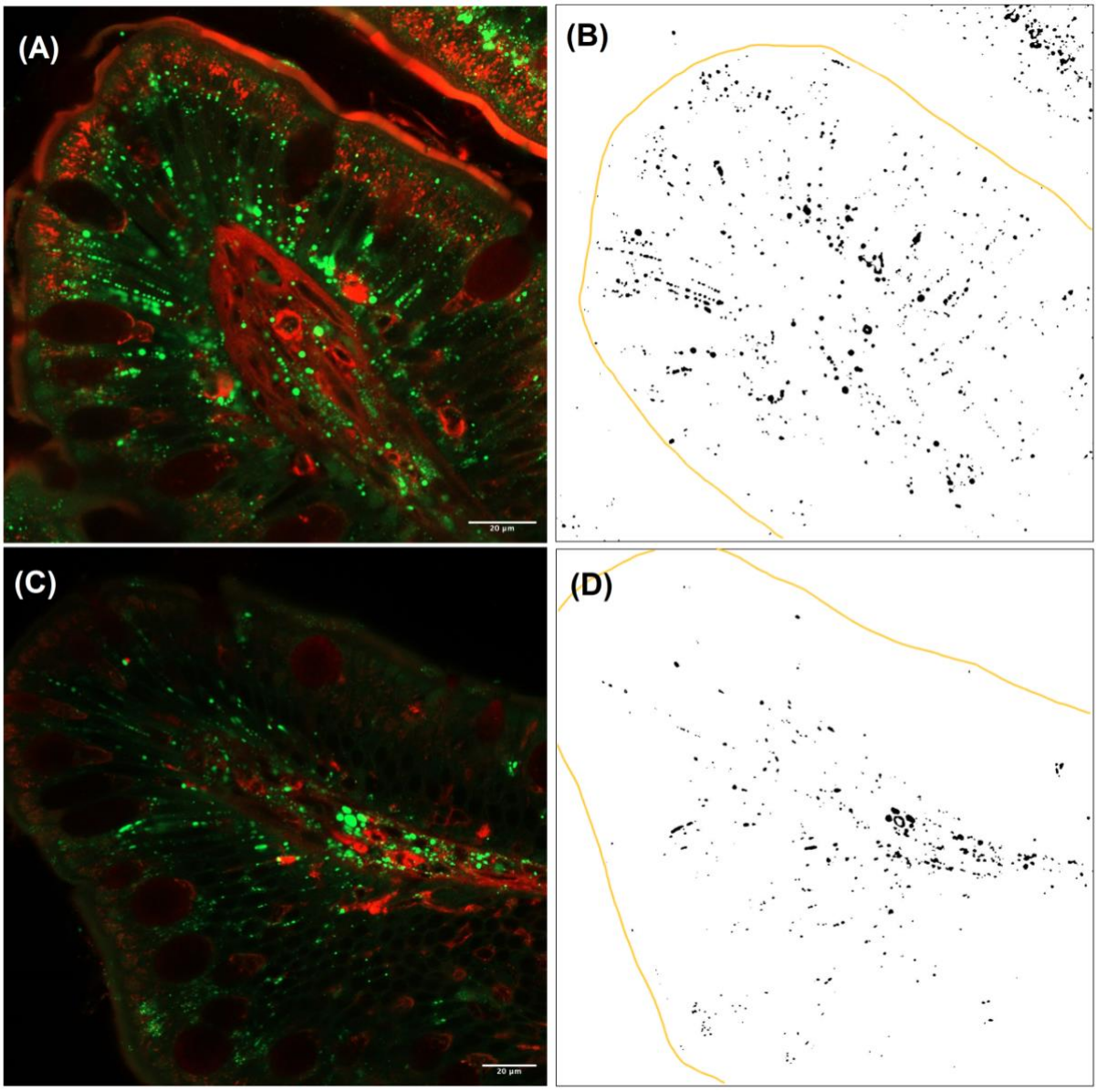

Figure 16: Bco1^{KO}-high Intestine

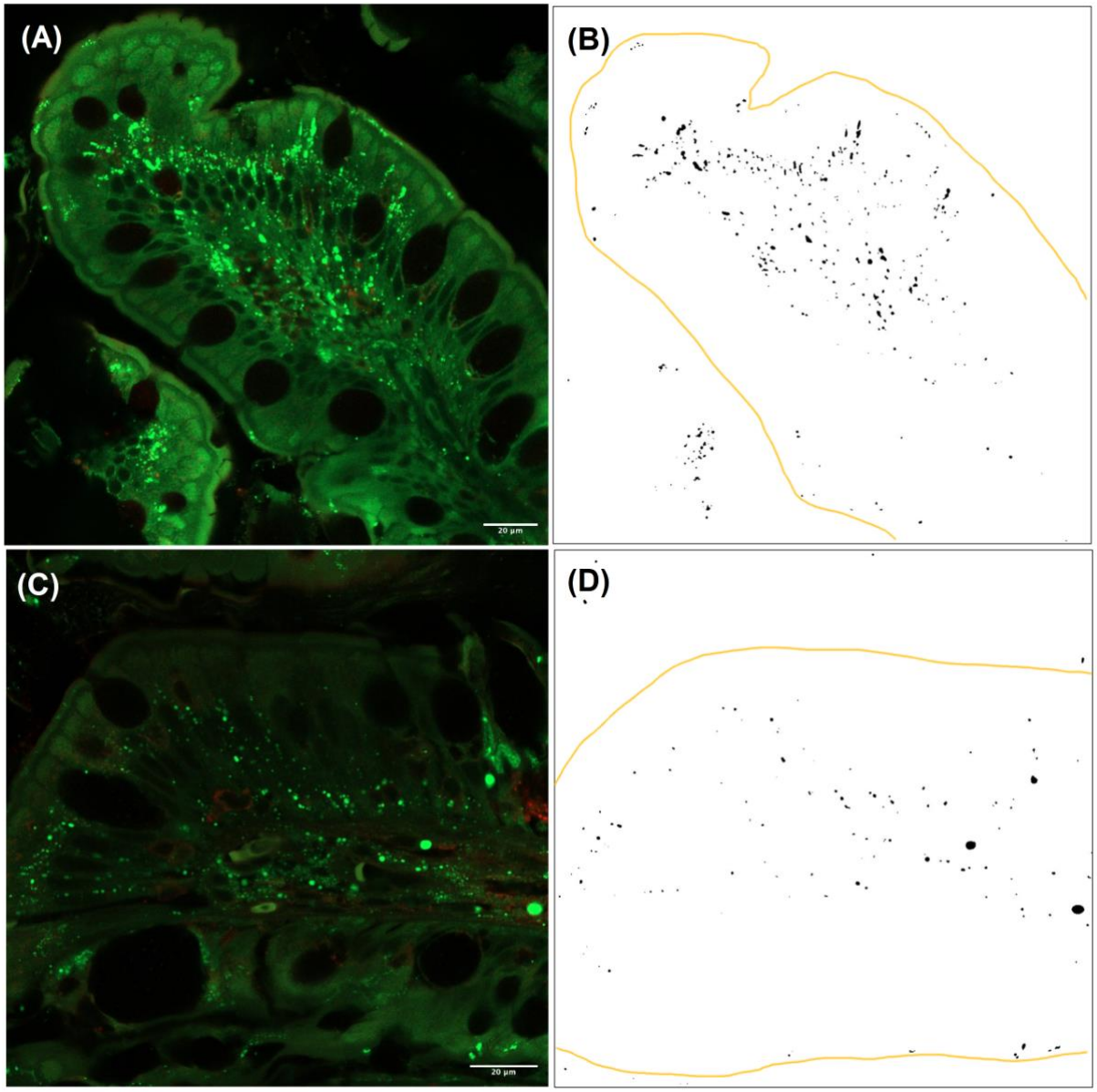

Figure 17: Bco1^{KO}-low Intestine

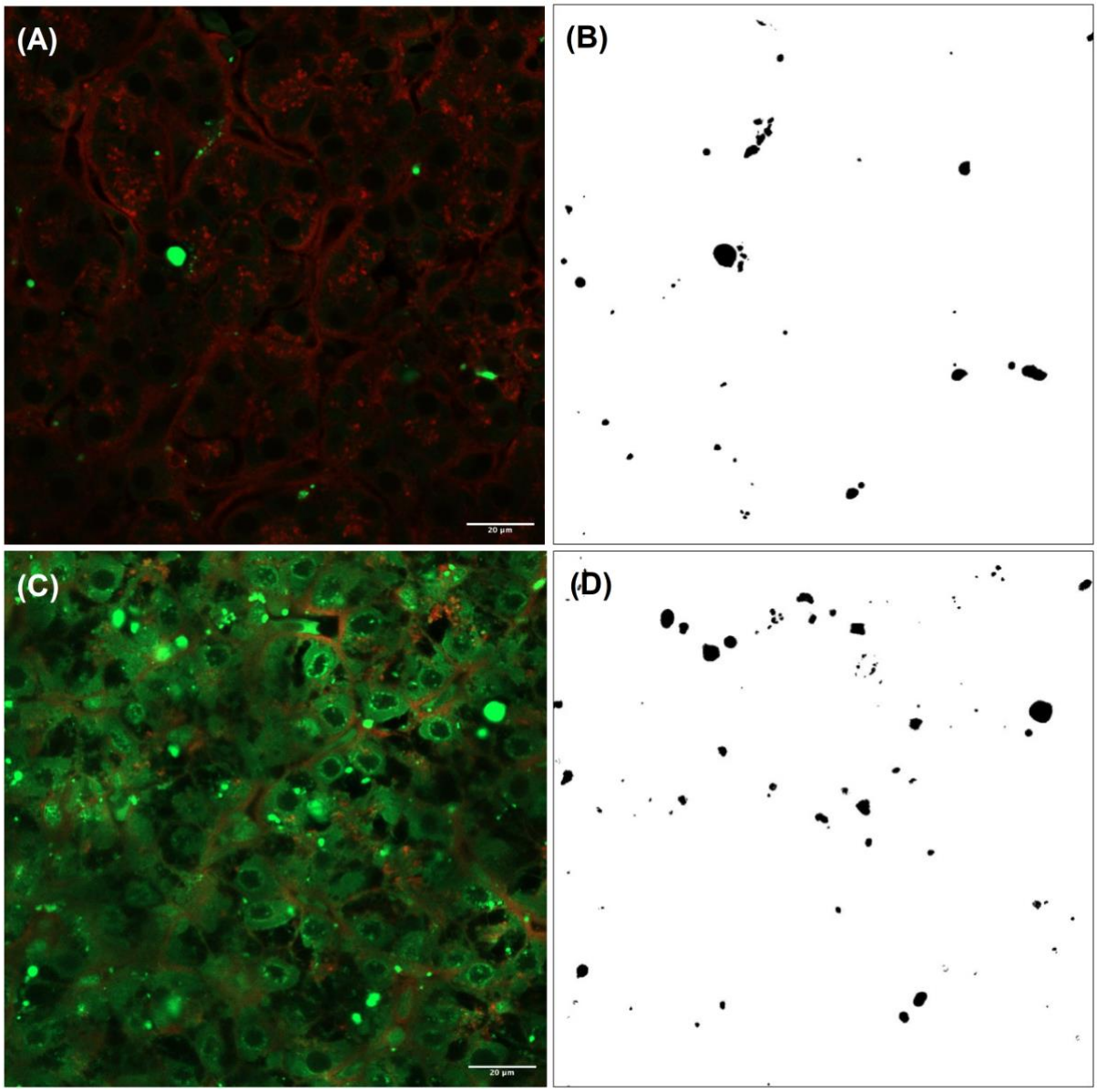

Figure 18: Control Liver

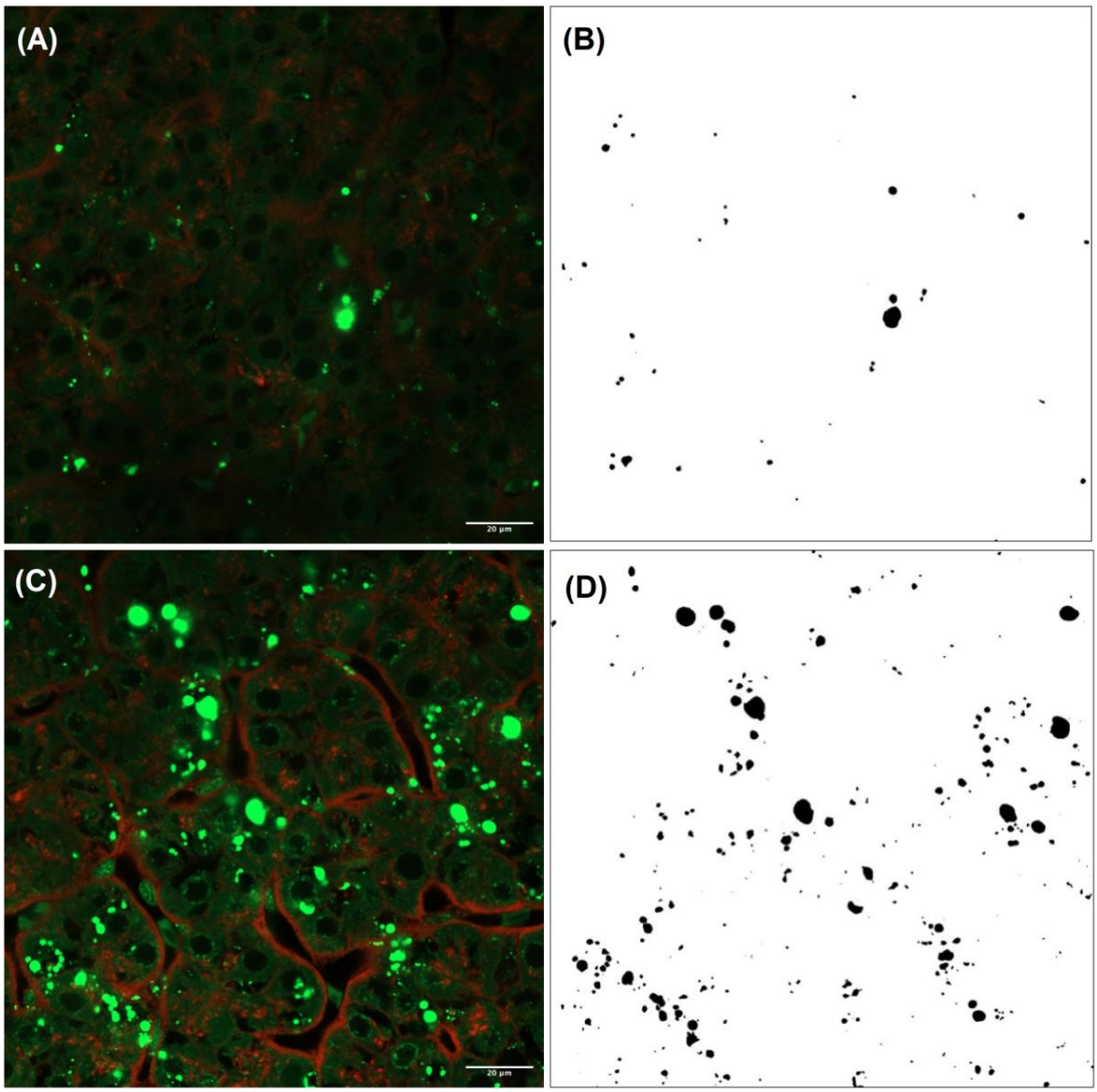

Figure 19: Abcg2^{KO} Liver

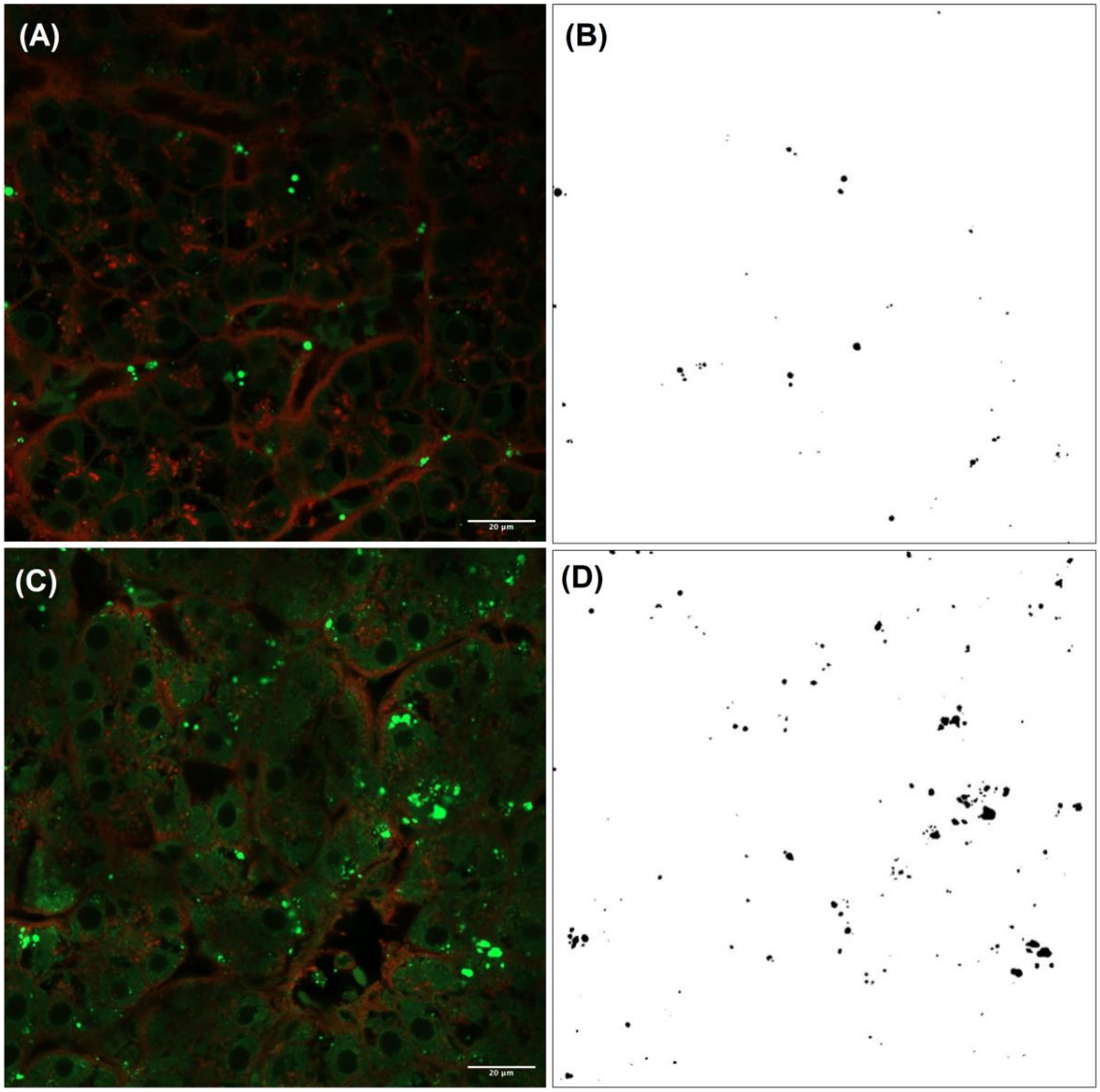

Figure 20: Bco1^{KO}-high Liver

m

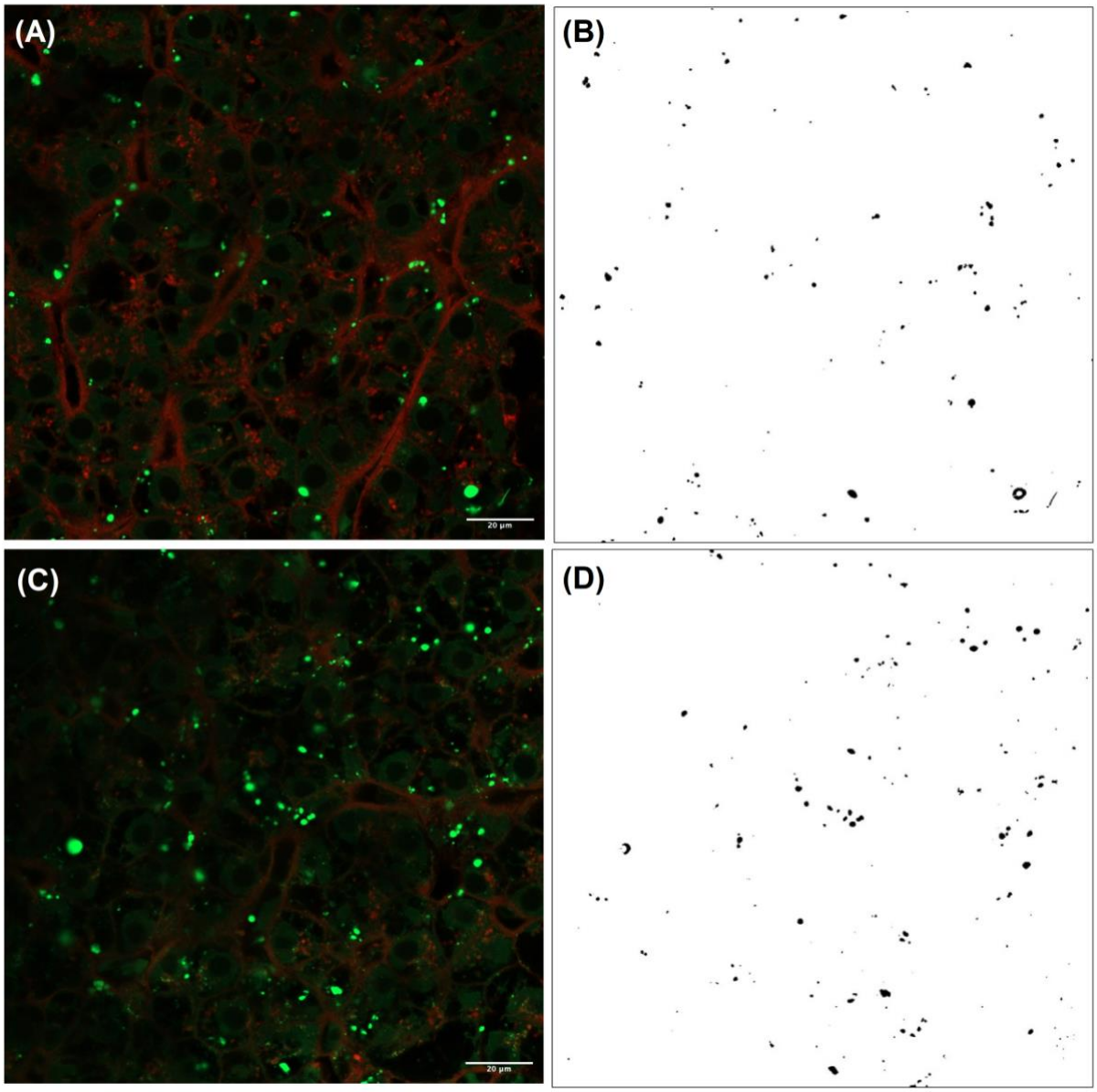

Figure 21: Bco1^{KO}-low Liver

n

Norges miljø- og biovitenskapelige universitet
Noregs miljø- og biovitskapelege universitet
Norwegian University of Life Sciences

Postboks 5003
NO-1432 Ås
Norway